

POTENTIAL OF USING LOW DENSITY LIPOPROTEINS  
(LDLs) AS CARRIERS OF RADIOIMAGING AGENTS  
FOR THE EARLY IDENTIFICATION OF  
ATHEROSCLEROTIC LESIONS AND  
CERVICAL CANCER CELL

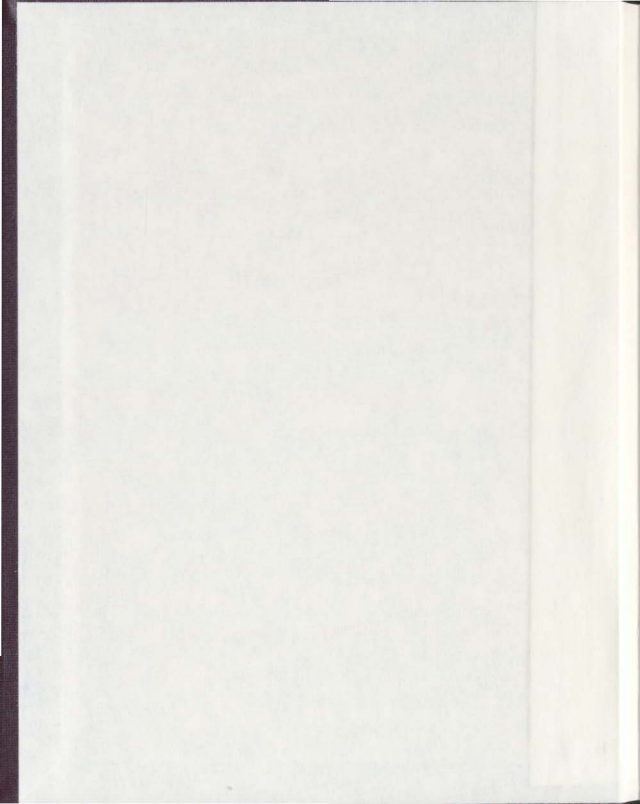
CENTRE FOR NEWFOUNDLAND STUDIES

---

**TOTAL OF 10 PAGES ONLY  
MAY BE XEROXED**

(Without Author's Permission)

WU XIAO







## NOTE TO USERS

Page(s) not included in the original manuscript and are unavailable from the author or university. The manuscript was scanned as received.

36, 57

This reproduction is the best copy available.

**UMI**<sup>®</sup>





National Library  
of Canada

Bibliothèque nationale  
du Canada

Acquisitions and  
Bibliographic Services

Acquisitions et  
services bibliographiques

395 Wellington Street  
Ottawa ON K1A 0N4  
Canada

395, rue Wellington  
Ottawa ON K1A 0N4  
Canada

*Your file* *Votre référence*

*ISBN: 0-612-84054-9*

*Our file* *Notre référence*

*ISBN: 0-612-84054-9*

The author has granted a non-exclusive licence allowing the National Library of Canada to reproduce, loan, distribute or sell copies of this thesis in microform, paper or electronic formats.

L'auteur a accordé une licence non exclusive permettant à la Bibliothèque nationale du Canada de reproduire, prêter, distribuer ou vendre des copies de cette thèse sous la forme de microfiche/film, de reproduction sur papier ou sur format électronique.

The author retains ownership of the copyright in this thesis. Neither the thesis nor substantial extracts from it may be printed or otherwise reproduced without the author's permission.

L'auteur conserve la propriété du droit d'auteur qui protège cette thèse. Ni la thèse ni des extraits substantiels de celle-ci ne doivent être imprimés ou autrement reproduits sans son autorisation.

**Canada**



**Potential of Using Low Density Lipoproteins  
(LDLs) as Carriers of Radioimaging Agents for the  
Early Identification of Atherosclerotic Lesions and  
Cervical Cancer Cells**

by

**Wu Xiao**

A thesis submitted to the School of Graduate Studies  
in partial fulfilment of the requirements  
for the degree of Master of Science

School of Pharmacy  
Memorial University of Newfoundland

August, 1999

St. John's      Newfoundland      Canada

## **Abstract**

Atherosclerosis is the underlying factor leading to such cardiovascular diseases (CVD) as stroke, aneurysm, and myocardial infarction. The early detection of atherosclerotic plaques is considered to be crucial for successful prevention and/or therapeutic and dietary intervention of CVD. Current diagnostic practice, on the other hand, can only detect the problem at an advanced stage. The purpose of the work in this thesis was to examine the potential of using non-hydrolyzable radioimaging agents /acetylated low density lipoprotein (AcLDL) conjugates as diagnostic drugs for the early and non-invasive detection of atherosclerosis and for the monitoring of the effects of drug therapy.

Cholesteryl iopanoate (CI), a cholesteryl ester analog, 1,3-dihydroxypropan-2-one 1,3-diiopanoate (DPIP), a diglyceride analog, and a new compound, cholesteryl 1,3-diiopanoate glyceryl ether (C2I), were synthesized, radiolabeled, and incorporated into AcLDL to use as radiotracers for testing their potential clinical use in the early diagnosis of atherosclerosis in experimental rabbits. Biodistribution of these agents was studied, and aortae of both atherosclerotic lesioned and control rabbits were removed for Sudan IV staining and autoradiography in order to confirm the formation of the atherosclerotic lesion and localization of radioactivity respectively.

The injected drugs were found to be cleared from blood following a two compartment model. All of the three drugs were shown to be resistant to hydrolysis

*in vivo*. Radioactivity in the atherosclerotic aorta was found to be significantly higher than that in normal aorta in terms of C1 and C21 compounds, suggesting that both of the proposed diagnostic probes were selectively taken up by the atherosclerotic lesions. The autoradiography and staining results confirmed that the localization of the proposed probes was superimposed with the atherosclerotic lesion site. Work in this regard was published in part (Xiao et al., 1999a) and summarized in Chapter 2.

Other work included in this thesis contains a method we developed in our lab to significantly enhance the drug loading efficiency into LDL using a microemulsion with seal oil as the major constituent (see Xiao et al., 1999b and Chapter 3 for details), and the research on the potential of using DPIIP loaded LDL as a tumor imaging agent for the detection of cervical tumors (see Xiao et al., 1999c and Chapter 4 for details).

## **Acknowledgement**

I would like to extend my sincere appreciation to my supervisor, Dr. Hu Liu, for his inspiring instructions and support through these two years of my Master's program. His attitude to science and devotion to research will leave a deep impression on me throughout my scientific career.

The author is also grateful to Dr. Alan Pater, my co-supervisor, and Dr. Lili Wang, my committee member. From them a great number of magnificent ideas, comments, and suggestions were received, which were critical to the accomplishment of my projects.

During the progress of my projects, Dr. Thomas Scott and Dr. Phil Davis generously helped me with their extraordinary research skills, excellent lab facilities, and outstanding scientific experience.

Special thanks to Mr. Zhongshui Yu and Ms. Liping Feng for their high quality and efficient assistance to my projects when I was in my busiest final stage of my Master's program and after I left Memorial University of Newfoundland.

Projects in this thesis were supported in part by funding from Banting Foundation and the Medical Research Council of Canada. The author was financially supported by the School of Graduate Studies, Memorial University of Newfoundland, Canada.

## TABLE OF CONTENTS

	Page
Title .....	i
Abstract .....	ii
Acknowledgment .....	iv
Table of Contents .....	v
List of Tables .....	vii
List of Figures .....	viii
Glossary of Abbreviations .....	x
Chapter 1. Introduction .....	1
Composition and Morphology of Plaque .....	2
Imaging Devices for Atherosclerosis .....	6
Radiotracers and Radioimaging of Atherosclerosis .....	10
Objectives .....	21
Chapter 2. Acetylated Low Density Lipoprotein as a Carrier to Deliver Radioimaging Probes for the Visualization of Early Atherosclerotic Lesions in Rabbits .....	24
Introduction .....	24
Materials and Methods .....	26
Results and Discussion .....	34
Conclusion .....	56
Chapter 3. Seal Oil Markedly Enhances the Transfer of a Hydrophobic	

Radiopharmaceutical into Acetylated Low Density Lipoprotein . . . .	57
Introduction . . . . .	57
Materials and Methods . . . . .	58
Results and Discussion . . . . .	62
Conclusion . . . . .	74
Chapter 4. Incorporation of an <sup>125</sup> I-labeled hexa-iodinated diglyceride analog into low density lipoprotein and high specific uptake by cervical carcinoma cell lines . . . . .	75
Introduction . . . . .	75
Materials and Methods . . . . .	77
Results . . . . .	80
Discussion . . . . .	92
Chapter 5. Conclusion . . . . .	96
References . . . . .	98

## List of Tables

Table I.	Radiotracers for imaging atherosclerosis . . . . .	11
Table II.	Comparison between atherosclerotic and control rabbits of cholesterol, triglyceride, HDL and LDL contents in blood . . . . .	40
Table III.	Pharmacokinetic parameters of the radioactivity in the blood of atherosclerotic and control rabbits after i.v. injection of $^{125}\text{I}\text{-Cl/AcLDL}$ at $2\mu\text{Ci/kg}$ dose . . . . .	42
Table IV.	Comparison between atherosclerotic and control rabbits of distribution of radioactivity in various tissues after i.v. injection of $^{125}\text{I}\text{-Cl/AcLDL}$ at $2\mu\text{Ci/kg}$ dose . . . . .	45
Table V.	Comparison between atherosclerotic and control rabbits of distribution of radioactivity in various tissues after i.v. injection of $^{125}\text{I}\text{-DPIP/AcLDL}$ at $2\mu\text{Ci/kg}$ dose . . . . .	49
Table VI.	Comparison between atherosclerotic and control rabbits of distribution of radioactivity in various tissues after i.v. injection of $^{125}\text{I}\text{-C2I}$ at $15\mu\text{Ci/kg}$ in the anti-atherogenic agent group, cholesterol group, and control group rabbits . . . . .	54
Table VII.	Maximum number of binding sites ( $B_{\text{max}}$ ) and equilibrium dissociation constant ( $K_d$ ) for LDL receptor-mediated binding of LDL to cervical carcinoma cells . . . . .	87

## List of Figures

Figure 1.	Classification of coronary atherosclerotic lesions in terms of its phases, morphology and histopathology.....	4
Figure 2.	Structure of cholesteryl iopanoate (CI) .....	20
Figure 3.	Structure of 1,3-dihydroxypropan-2-one 1,3-diiopanoate (DPIP) .....	20
Figure 4.	Structure of cholesteryl 1,3-diiopanoate glyceryl ether (C2I) .....	20
Figure 5.	Synthesis of cholesteryl 1,3- diiopanoate glyceryl ether (C2I) . .....	30
Figure 6.	Chromatograms of gel filtration of $^{125}\text{I}$ -CI/AcLDL conjugates monitored for radioactivity and protein .....	37
Figure 7.	Distribution of radioactivity upon incubation of $^{125}\text{I}$ -CI/AcLDL with plasma .....	38
Figure 8.	Amount of $^{125}\text{I}$ -CI in blood versus time after i.v. injection of $^{125}\text{I}$ -CI at 2 $\mu\text{Ci}/\text{kg}$ in atherosclerotic and control rabbits .....	41
Figure 9.	Distribution of radioactivity in various tissues in atherosclerotic and control rabbits after i.v. injection of $^{125}\text{I}$ -CI/AcLDL at 2 $\mu\text{Ci}/\text{kg}$ . . . . .	44
Figure 10.	Correlation between Sudan IV staining results and autoradiography - CI .....	46
Figure 11.	Distribution of radioactivity in various tissues in atherosclerotic and control rabbits after i.v. injection of $^{125}\text{I}$ -DPIP/AcLDL at 2 $\mu\text{Ci}/\text{kg}$ .....	50
Figure 12.	Biodistribution of $^{125}\text{I}$ -C2I in the anti-atherogenic agent group, cholesterol group, and control group rabbits .....	53

Figure 13.	Correlation of Sudan IV staining and autoradiography -C2I.....	55
Figure 14.	Comparison of DPIP concentrations in microemulsions prepared using triolein, canola oil, squalene or seal oil as the core lipid component. .....	65
Figure 15.	Electron micrographs of DPIP microemulsions prepared using triolein, canola oil, squalene or seal oil as the core lipid component .....	66
Figure 16.	Image analysis of DPIP microemulsions prepared using triolein, canola oil, squalene, or seal oil, respectively, as the core lipid component....	67
Figure 17.	Confirmation of <sup>125</sup> I-DPIP incorporation into AcLDL particles prepared using three different lipid microemulsions .....	70
Figure 18.	Comparison of the DPIP loading efficiency into AcLDL using different methods .....	73
Figure 19.	Confirmation of <sup>125</sup> I-DPIP incorporation into LDL particles .....	82
Figure 20.	HeLa cell LDL receptor-mediated <sup>125</sup> I-LDL binding at 4 °C .....	84
Figure 21.	SiHa cell LDL receptor-mediated <sup>125</sup> I-LDL binding at 4 °C .....	85
Figure 22.	C-33A cell LDL receptor-mediated <sup>125</sup> I-LDL binding at 4 °C .....	86
Figure 23.	HeLa cell LDL receptor-mediated <sup>125</sup> I-LDL uptake at 37 °C .....	89
Figure 24.	SiHa cell LDL receptor-mediated <sup>125</sup> I-LDL uptake at 37 °C .....	90
Figure 25.	C-33A cell LDL receptor-mediated <sup>125</sup> I-LDL uptake at 37 °C .....	91

## **Glossary of Abbreviations**

<b>AcLDL</b>	Acetylated low density lipoprotein
<b>Apo</b>	Apolipoprotein
<b>BPD</b>	Benzoporphyrin derivative
<b>BSA</b>	Bovine serum albumin
<b>C2I</b>	1,3- diiopanoate glyceryl ether
<b>CE</b>	Cholesteryl ester
<b>CETP</b>	Cholesteryl ester transfer protein
<b>cpm</b>	Counts per minutes
<b>CI</b>	Cholesteryl iopanoate
<b>CT</b>	Computer tomography
<b>CVD</b>	Cardiovascular disease
<b>DPIP</b>	1,3-dihydroxypropan-2-one 1,3-diiopanoate
<b>DPPC</b>	Dipalmitoyl L- $\alpha$ -phosphatidylcholine
<b>DPPE</b>	Dipalmitoyl DL- $\alpha$ -phosphatidylethanolamine
<b>EBCT</b>	Electron beam CT
<b>EM</b>	Electron microscopy
<b>FCS</b>	Fetal calf serum
<b>FDG</b>	Fluorodeoxyglucose
<b>HDL</b>	High density lipoprotein
<b>HPLC</b>	High performance liquid chromatography

LDL	Low density lipoprotein
LPDS	Lipoprotein deficient serum
MRA	Magnetic resonance angiography
MRI	Magnetic resonance imaging
OxLDL	Oxidized low density lipoprotein
PBS	Phosphate buffered saline
PET	Positron emission tomography
SDS-PAGE	Sodium dodecyl sulfate polyacrylamide gel electrophoresis
SPECT	Single photon emission tomography
TLC	Thin layer chromatography
VLDL	Very low density lipoprotein

## **Chapter 1. Introduction**

Atherosclerosis is a long-term, progressive disease of blood vessels with cellular and metabolic alterations, including cellular proliferation and accumulation of low-density lipoproteins (LDL) in the mural arteries (Ross, 1993). In most cases of atherosclerosis the elastic arteries (aorta, carotid and iliac) and some of the large- and medium-sized muscular arteries (coronary and popliteal) are pathologically changed. The coronary arteries, the popliteal arteries, the descending thoracic aorta, the internal carotid arteries and the vessels of circle of willis are some of the most severely involved vessels. More specifically, coronary carotid, cerebral arteries and the aorta are the prime foci of atherosclerotic complications, and as a result, thrombotic myocardial infarction, thromboembolic cerebral infarction and aortic aneurysms are the major consequences of this disease.

It takes decades to develop the mature atherosclerotic plaques that will cause the clinical complications, such as thrombotic and thromboembolic occlusion and aneurysms. Atherosclerosis is the leading cause of morbidity and mortality in the Western world, and nearly 50% of all deaths in the U.S. are generally attributed to diseases associated with atherosclerosis. Therefore, quantitative assessment of atherosclerotic or atherothrombotic disease during its evolution and after therapeutic interventions is important for understanding the progression of the disease and for selecting appropriate medicinal or surgical measures.

Many invasive and noninvasive imaging techniques have been available for

detecting characteristics of vascular lesions. Before introducing these detection methods, some description of atherosclerotic plaque composition and morphology would be helpful.

### **Composition and Morphology of the Plaque**

Typically the mature atherosclerotic plaques consist of the lipid-rich atheromatous gruel and collagen-rich sclerotic tissue (Falk et al., 1995). The basic lesion appears white or whitish yellow and consists of a raised focal plaque which contains a lipid core and a covering fibrous cap within the intima. The core within the plaque contains crystalline cholesterol, cholesteryl esters, phospholipids, cellular degradation products and collagen remnants (Stary et al., 1994; Stary et al., 1995). The fibrous cap covering the core is composed of smooth muscle cells, macrophages and collagen contents. As the plaque grows, the lumen of the artery is encroached with stenosis. The morphological features of atherosclerotic lesions are characterized by lesion length, smoothness of lumen outline, eccentricity of the lumen, abrupt or tapered shoulders, defects due to thrombus, and the presence of calcification. Current knowledge about the pathophysiology and progression of atherosclerosis has suggested that the composition and vulnerability to pathology of the plaque is related to the clinical status of the patient, and the sudden conversion of a stable atherosclerotic plaque to an unstable and life-threatening atherosclerotic lesion or vulnerable plaque is caused by plaque fissuring, rupture or

disruption (Falk and Fernandez-Ortiz, 1995; Maximilian and Willerson, 1994; Kaartnen et al., 1994).

According to the criteria set forth by the American Heart Association Committee on Vascular Lesions, plaque progression in coronary arteries can be subdivided into five phases and various lesion types, as shown in Figure 1 (Stary et al., 1994; Stary et al., 1995). Phase 1 lesions can usually be found in people younger than 30. Such small lesions may progress over a period of years and are categorized as type I, II and III lesions. Phase 2 indicates plaques that, although not necessarily stenotic, may be prone to disruption because of high lipid content. The lesions are categorized as type IV or Va. Phase 2 can proceed into acute phase 3 or 4, and both of these can evolve into fibrotic phase 5. Phase 3 consists of the acute type VI lesions with a mural thrombus that could possibly occlude the artery. Phase 4 consists of the acute complicated type VI lesion with an occlusive thrombus, which may result in an acute coronary syndrome.

Figure 1. Classification of coronary atherosclerotic lesions in terms of their phases, morphology and histopathology.

	Lesion Type	Lesion Morphology	Clinical Symptoms
Phase 1	I	Foam cells	No symptoms
	II	Foam cells, smooth muscle cells and extracellular lipid droplets	
	III	Smooth muscle cells surrounded by extracellular connective tissue, fibrils and lipid deposits	
Phase 2	IV	Confluent cellular lesions with a great deal of extracellular lipid, intermixed with fibrous connective tissue	
	Va	Extracellular lipid covered by thin fibrous cap	
Phase 3	VI	Disruption of type IV and Va lesions with a mural thrombus that may or may not occlude the artery	
Phase 4	VI	Disruption of type IV or Va lesions with occlusive thrombus	Acute syndromes, myocardial infarction, unstable angina, ischemic sudden death
Phase 5	Vb-Vc	Changes in geometry of the disrupted plaque, and organization of mural thrombus by connective tissue may lead to formation of occlusive and fibrotic type of lesions	Silent occlusive process or Angina pectoris

In Phase 5, changes in the shape of disrupted plaques and the organization of connective tissues can lead to the more occlusive and fibrotic type Vb or Vc lesions. These occlusive lesions can be clinically silent or produce angina.

Coronary occlusion and myocardial infarction are most frequently developed from mild-to-moderate stenosis of lipid-rich lesions. It has been observed that acute ischemic events are due to the disruption of lipid-rich lesion types IV and Va, which are often invisible to angiography. Therefore, the imaging of less obstructive lipid-rich plaques vulnerable to rupture would be valuable for clinical interventions. While they are in carotid arteries, the vulnerable plaques are severely stenotic and appear to be ulcerated and disrupted. Once the fibrous cap in lipid-rich coronary plaques disintegrates, tears or breaks and exposes the thrombogenic gruel to the flowing blood, a type IV or Va lesion suddenly evolves into an acute complicated type VI lesion (Falk and Fernandez-Ortiz, 1995). In contrast, the vulnerable carotid plaques are heterogeneous and stenotic. Their rupture or dissection probably relates to the impact of blood flow.

Plaques containing large and soft cores of liquid cholesterol esters are highly vulnerable to rupture and thrombosis (Falk and Fernandez-Ortiz, 1995). On the contrary, hard sclerotic plaques with a high content of smooth muscle cells and collagen are less susceptible for rupture. Fibrous caps vary widely in thickness, cellularity, matrix, strength and stiffness. The thinnest parts of them are usually at their shoulder regions, where macrophages accumulate and disruption often occurs

(Moreno et al., 1994). *In vitro* studies suggest that infiltration of macrophage and their release of metalloproteinases weakens the caps locally (Galis et al., 1995).

### **Imaging Devices for Atherosclerosis**

Several invasive and noninvasive devices or instruments are routinely used to identify atherosclerosis and to assess the progression of the disease. Most of the standard techniques measure the morphological parameters of the atherosclerosis, including the decrease of the luminal diameter or stenosis and the increase of the wall thickness, and provide qualitative or semiquantitative assessment of the relative risk associated with the disease. These techniques will be described in the following context:

Angiography is used to reveal the luminal diameter and provide a measure of stenosis with excellent resolution, but not to image the vessel wall and its various histopathological components. This technique is most widely employed for the diagnosis of coronary (Galis et al., 1995; Ambrose, 1996), carotid (Kohler, 1996) and peripheral artery (Dinsmore and Rivitz, 1996) lesions, and is the "gold standard" for anatomic diagnosis despite limited specificity and sensitivity.

Angioscopy is a method for the visualization of the arterial wall rather than lumen. It reveals the plaque and surface features that are not seen angiographically (Den Heijer et al., 1994; Uchida et al., 1995). In addition, it is able to show the color of the materials in the artery, and it therefore is highly sensitive for the detection of

thrombus. However, since it views only the lesion surface, it cannot present the internal heterogeneity of the plaque. As a routine clinical tool, it may not be practical due to the thickness of the catheter.

Catheter-based ultrasound is a new approach to the imaging of vascular anatomy. This technique permits direct imaging of atheroma and provides a cross-sectional, tomographic perspective of the vessel and the atherosclerotic disease (Nissen et al., 1996; Von Birgelen et al., 1995; Roelandt et al., 1994). The diagnostic applications of intravascular ultrasound include the detection of angiographically unrecognized disease, detection of lesions of uncertain severity (40%-75% stenosis) and risk stratification of atherosclerotic lesions in interventional practice.

A major cause of ischemic cerebrovascular disease is extracranial carotid atherosclerosis, because stroke and transient ischemic attacks are commonly associated with advanced atherosclerosis at the carotid bifurcation (Kohler, 1996). Duplex imaging (B-mode ultrasound) is typically used to detect extracranial carotid atherosclerosis due to its noninvasiveness. Clinically, it has been used to evaluate the efficacy of drugs and study the natural history of atherosclerosis (longitudinal studies) by follow-up individuals at increased risk of atherosclerosis (Eliasziw et al., 1995).

Calcification of atherosclerotic lesions is an organized and regulated process and is found more frequently in advanced plaques (Wexler et al., 1996). A clear association between coronary calcium and obstructive coronary artery disease has been established, and it was clearly shown that the amount of coronary calcium was

a useful indicator of the extent of coronary artery disease (Agatston et al., 1990). Electron beam computer tomography (EBCT), magnetic resonance imaging (MRI), fluoroscopy, and helical CT are frequently used to identify calcific deposits in blood vessels, of which, however, only EBCT can quantitate the amount or volume of calcium (Wexler et al., 1996). EBCT detects the presence and progression of atherosclerotic lesions in the pre-complicated stage by monitoring the presence of coronary artery calcium (Janowitz et al., 1993).

Similar to conventional angiography techniques, magnetic resonance techniques use gradient echo methods to generate images of flowing blood as positive contrast within the lumen of the vessel (Doyle and Pohost, 1996; Grist and Turski, 1996). Magnetic resonance angiography (MRA) of coronary arteries is currently under development, and the resolution is in the range of 1 mm<sup>3</sup>. MRA techniques provide images of the vessel lumen, whereas MRI aims at evaluating the effects of the disease on the tissue supplied by the vessel. It has been reported that MRI techniques are valuable for studying the progression of experimental atherosclerosis in hypercholesterolemic rabbits and for imaging the plaque components such as fibrous caps, necrotic cores and intraplaque hemorrhage (Skinner et al., 1995).

Based on the above summary of the non-radioactive imaging techniques, the traditional "gold standard", angiography, detects advanced lesions and provides a measure of the degree of stenosis. Angioscopy, on the other hand, clearly identifies the presence of thrombus. These techniques, however, are ineffective in

determining which plaques are unstable and vulnerable to thrombosis and proliferation. In carotid arteries and arteries in lower extremities, duplex ultrasonography is useful for providing the degree of stenosis as well as plaque morphology, and for assessing changes in wall thickness. Although appearing to be the only clinically useful technique in imaging the unstable, vulnerable plaques in coronary arteries, intravascular ultrasound however is very invasive, like angiography and angioscopy, and is, therefore, not practical in evaluating the progression of atherosclerotic disease in patients with stable angina. MRA, being noninvasive, may replace angiography for anatomical imaging of the vasculature, but the MRA technique is also ineffective in imaging the vulnerable plaques. In the near future, magnetic resonance imaging techniques may be able to image vulnerable plaques and characterize plaques in terms of lipid and fibrous content and identify the presence of thrombus associated with the plaques. Ultrafast EBCT is noninvasive and useful for measuring the calcium content in the coronary arteries, but a good correlation between calcium concentration and plaque vulnerability has not been confirmed in clinics. Considering all the imaging devices used to detect the plaques at relatively advanced phases, radioimaging of the atherosclerosis at its early stages in which no symptom is clinically shown provides us a new noninvasive approach to the visualization of the lesions for identification and treatment purposes.

## **Radiotracers and Radioimaging of Atherosclerosis**

The principal mechanisms involved in human atherogenesis are lipid infiltration, cellular invasion and proliferation and thrombus formation. In the last 20 years, various radiotracers have been developed based on several molecules and cells involved in atherogenesis, and the potential diagnostic utility of these radiotracers for imaging atherosclerotic lesions has been studied by many investigators in animal models (Sinzing and Virgolini, 1990; Kritz et al., 1996; Strauss, 1996). These radiotracers are categorized into seven classes (Table I) and will be described in detail as follows.

Table I. Radiotracers for imaging atherosclerosis

	Categories of radiotracers	Radiotracers
Native products	Immunogloblins	
	Nonspecific	<sup>111</sup> In-DTPA-human polyclonal IgG (may bind to Fc receptors on macrophages)
	Specific monoclonal	<sup>111</sup> In-(DTPA-PL)-Z2D3 F(ab') <sub>2</sub> IgM (antibody against smooth muscle cells)
	Specific	<sup>131</sup> I-anti-ICAM-1 monoclonal IgG (antibody against endothelial adhesion molecule)
	Low Density Lipoprotein (LDL)	<sup>125</sup> I- or <sup>131</sup> I- or <sup>123</sup> I-LDL, <sup>111</sup> In-LDL, <sup>99m</sup> Tc-LDL and <sup>99m</sup> Tc-ox-LDL
	Peptides	<sup>123</sup> I-SP-4, <sup>99m</sup> Tc-P199 and <sup>99m</sup> Tc-P215 (peptides based on apo B-100)
	Monocytes	<sup>111</sup> In-monocytes
Radiochemicals	Metabolic tracer	<sup>18</sup> F-fluorodeoxyglucose (FDG) (may reflect macrophage density)
	Photosensitizer	Benzoporphyrin derivative (BPD) monoacid ring A
	Endogenous Lipid Analogs	<sup>125</sup> I-cholesteryl lopanoate ( <sup>125</sup> I-CI), <sup>125</sup> I-1,3-dihydroxypropan-2-one 1,3-diioanoate ( <sup>125</sup> I-DPIP), and <sup>125</sup> I-cholesteryl 1,3-diioanoate glyceryl ether ( <sup>125</sup> I-C2I)

Foam cells derived from macrophages are found in great amount in the fatty streaks and vulnerable plaques. It has been hypothesized that radiolabeled immunoglobulin, IgG, would be an appropriate radiotracer to image the Fc receptors on these cells in the atherosclerotic areas (Fischman et al., 1989). In patients with carotid atherosclerosis,  $^{111}\text{In}$ -labeled IgG identified 86% of the lesions determined by ultrasonography. However, it did not correlate with plaque morphology and clinical stage of the disease, as determined by ultrasound (Sinzing et al., 1996). Failure of detecting the early lesions in the aorta of Watanabe heritable hyperlipidemic rabbits using  $^{111}\text{In}$ -IgG was reported, possibly because of the slow plasma clearance of the tracers and high target-to-blood ratios for visualizing coronary artery lesions. The clinical and animal data clearly suggest that the accumulation of the tracer in the lesion may be nonspecific, and radiolabeled IgG may not be an appropriate radiotracer to image and identify vulnerable atherosclerotic lesions (Sinzing et al., 1996).

To overcome the problem of nonspecific localization of IgG, various monoclonal antibodies were developed against different cells and antigens present in the atherosclerotic lesions. Smooth muscle cells proliferation is one of the major signals of atherosclerotic disease. A mouse/human chimeric monoclonal IgM antibody fragment, Z2D3 F(ab')<sub>2</sub> IgM, with specificity for an antigen associated with smooth muscle cells was therefore developed (Narula et al., 1995).  $^{111}\text{In}$ -(DTPA-PL)-Z2D3 F(ab')<sub>2</sub> IgM-negative charge-modified antibody fragments were shown to

localize in experimental atherosclerotic lesions (Carrio et al., 1995).

Focal LDL accumulation in the arterial lesions is predominantly seen in the edges of regenerating endothelial islands, as reported in a study on balloon catheter-deendothelialized aorta of a rabbit (Chang et al., 1992). In 1983, Lees et al. (Lees et al., 1983) first demonstrated the diagnostic use of radiolabeled LDL for imaging carotid atherosclerotic lesions in patients. Subsequently, LDL was labeled with other radionuclides with different physical half-lives, such as  $^{123}\text{I}$ ,  $^{99\text{m}}\text{Tc}$  and  $^{111}\text{In}$ , and the uptake in atherosclerotic lesions was demonstrated in a variety of hypercholesterolemic rabbit models (Sinzinger and Virgolini, 1990; Vallabhajosula et al., 1988; Rosen et al., 1990) and in clinical studies (Lees et al., 1988; Virgolini et al., 1991; Vallabhajosula and Goldsmith, 1990; Ginsberg et al., 1990; Pirch and Sinzinger, 1995). It was observed in patients with carotid atherosclerosis that the uptake of  $^{99\text{m}}\text{Tc}$ -LDL occurred mostly in soft, macrophage-rich lesions, whereas the mature fibrocalcific plaques did not accumulate radiolabeled LDL (Lees et al., 1988; Virgolini et al., 1991). Some other experiments also showed that macrophage-rich tissues, including the tendon xanthomas in hypercholesterolemic patients and the expanded bone marrow in myeloproliferative patients, cumulated extensive quantity of radiolabeled LDL (Vallabhajosula and Goldsmith, 1990; Ginsberg et al., 1990). Even though the potential for diagnostic imaging of radioiodinated LDL and  $^{99\text{m}}\text{Tc}$ -LDL was demonstrated in patients with carotid and femoral atherosclerosis (lesion types III-V), clinical use of this technique remains elusive. In coronary arteries,  $^{99\text{m}}\text{Tc}$ -LDL imaging does not detect lesions for two reasons: the absolute and specific

uptake of radiotracer in the lesion is very low (<0.1% of the injected dose), and the blood-pool activity is very high due to slow plasma clearance of the radiotracer.

Many studies have demonstrated that chemically modified LDLs, such as oxidized LDL (OxLDL) and acetylated LDL (AcLDL) can be taken up by macrophages more efficiently than native LDL (Ross, 1993). Therefore, OxLDL or AcLDL labeled with appropriate radionuclides would be expected to be more selective than radiolabeled native LDL for imaging atherosclerotic lesions *in vivo*. However, some studies on both patients and animals indicated that although <sup>99m</sup>Tc uptake in carotid lesions was slightly greater when labeled on OxLDL than it was on native LDL, there were no significant differences between the two tracers in terms of their lesion detectability, even though the blood clearance of LDL is enhanced due to oxidation (Luliano et al., 1996). In the mean time, the aortic focal uptake of modified LDL was similar to that of native LDL, suggesting that the focal uptake of LDL in arterial lesions is mediated by specific, oxidation-independent patterns of charge and polarity (Chang et al., 1993). No report on using radiolabeled AcLDL for the detection of atherosclerotic lesions has yet appeared.

In another recent animal study (Yancey and Jerome, 1998), however, it was reported that heavily oxidized LDL will result in the LDL containing almost no free cholesterol or cholesteryl ester. This may partly explain why in the above research there was no difference in the specificities of OxLDL and LDL. This study also suggested that mildly oxidized LDL was better than AcLDL in terms of its localization on macrophages (Yancey and Jerome, 1998).

Due to the long circulation time of lipoproteins in the blood, the target-to-background ratio is much higher, which hinders the utilization of them as radio tracers. Some small peptides, normally 10-20 amino acids, by contrast are cleared from the circulation very rapidly. Therefore, they can provide high target-to-background ratios within minutes after injection. Based on the structure of apo B-100 protein of LDL, the first synthetic peptide, SP-4, was developed in 1990 (Shih et al., 1990). In later reports, radioiodinated SP-4 showed significant accumulation in experimental atherosclerotic lesions (Hardoff et al., 1993). Since then, other synthetic peptides have been developed (P-199 and P-215) and radiolabeled with  $^{99m}\text{Tc}$  (Vallabhajosula et al., 1993). The principal advantage of  $^{99m}\text{Tc}$ -labeled peptides compared to  $^{99m}\text{Tc}$ -LDL is that imaging can be performed within 1 hour postinjection because the peptides are cleared much faster than LDL from the circulation. In pilot studies involving patients with carotid atherosclerotic lesions documented by ultrasound,  $^{99m}\text{Tc}$ -P215 single photon emission computer tomography (SPECT) images showed some uptake in the atherosclerotic lesions immediately postinjection (Lees and Lees, 1996). In conditions associated with endothelial cell injury, the peptide endothelin has been shown to present in vascular smooth muscle cells and endothelial cells of human atherosclerotic lesions. Radioiodinated endothelin was shown to accumulate in experimentally induced arterial wall injuries in rabbits (Prat et al., 1993). Recently, several endothelin derivatives have been labeled with  $^{99m}\text{Tc}$  and have been shown to accumulate in significant amounts in experimental atherosclerotic lesions in rabbits (Dinkelborg et

al., 1995).

The conventional nuclear medicine gamma cameras have a resolution of 1.0-1.5 cm for planar and SPECT imaging techniques. In contrast, the positron emission tomography (PET) cameras provide 4-5 mm of resolution. <sup>18</sup>F-labeled FDG, an analog of glucose, has been used extensively as a radiotracer to estimate glucose metabolic rates of brain, heart and tumor tissues (Phelps et al., 1978; Strauss and Conti, 1991). This analog competes with glucose for transport into the cell and is subsequently trapped within the cell. While investigating the mechanisms of FDG accumulation in tumor tissue, Kubota et al. (Kubota et al., 1994) reported that, within the tumor, the uptake of deoxyglucose by macrophages was higher than that by tumor cells. Because atherosclerotic lesions are rich in macrophages, it was hypothesized that FDG-PET imaging of atherosclerosis may provide a noninvasive test to image and quantify the extent of macrophage content in an atherosclerotic lesion. This metabolic tracer showed significant localization in experimental atherosclerotic lesions of hypercholesterolemic rabbits (Vallabhajosula et al., 1996). In addition, histopathological data suggest that the amount of FDG uptake in the lesion correlates with the macrophage density in the lesion (Vallabhajosula et al., 1996). Because FDG clears from circulation rapidly, FDG-PET scans may provide excellent image quality with very high target-to-background ratios within 30 min postinjection, although the high cost of the instrumentation may compromise its uses.

The rationale for the use of photosensitizers in the treatment of peripheral

atherosclerosis is based upon the selective uptake and retention of the photosensitizer by atherosclerotic plaque as compared to the adjacent normal arterial tissue (Kessel and Sykes, 1984; Spokojny et al., 1986). Light activation of the photosensitizer only at the affected site would further increase the specificity of treatment. Thus, for photodynamic therapy to be applied to the treatment of peripheral atherosclerosis, delivery of the photosensitizers to abnormal vascular tissue must be optimized. Allison et al. (Allison et al., 1997) found that preassociation with LDL and AcLDL enhanced accumulation of a benzoporphyrin derivative, a photosensitizer, in atherosclerotic tissue when compared with normal artery, indicating that light activation could lead to a highly selective destruction of diseased vascular tissues.

A common drawback of all radiolabeled native products, including LDLs, peptides, and immunoglobulins is that once these radiotracers are taken up by the target tissues, they will be quickly degraded within the lysosomal compartment inside the cell and then be excreted, which compromises the selectivity of these targeting tracers for long-term monitoring. Unhydrolyzable radiochemicals, however, can be induced to be internalized to the target sites and entrapped in these cells for a long period for observation purposes. Cholesteryl iopanoate (CI) was a compound synthesized in Dr. Counsell's lab at University of Michigan (Figure 2). This compound simulates the structure of natural cholesteryl esters (CEs), which are the major components of LDL core, and was reported to be resistant to *in vivo* hydrolysis (DeGalan et al., 1986). In addition, each CI molecule bears three iodines, which

provides it a great potential for a high specific radioactivity after these iodines are exchanged by their radioactive counterparts, such as  $^{125}\text{I}$ ,  $^{131}\text{I}$ , and  $^{123}\text{I}$ . A series of tests of radioiodinated CI on its ability to follow the natural lipid deposit procedure at the atherosclerotic lesion sites for the purpose of early detection were performed by formulating this compound in saline (DeForge et al., 1989; DeGalan et al., 1986; DeGalan et al., 1988). However, due to the lack of the selectivity,  $^{125}\text{I}$ -CI formulated with saline was not successfully demonstrated to be a promising diagnostic agent for the early visualization of atherosclerotic lesions.

In our lab recently, AcLDL was chosen to be an selective carrier to deliver  $^{125}\text{I}$ -CI into the plaque induced into New Zealand White rabbits' aortae (Xiao et al., 1999a). Because LDL, OxLDL and AcLDL have been demonstrated to have selectivity to atherosclerotic plaques (Luliano et al., 1996; Chang et al., 1993; Yancey et al., 1998; Allison et al., 1997), and the hydrophobic core of LDL provides a large space for retaining foreign hydrophobic compounds, loading labeled CI into LDL will both improve the targeting specificity for CI and avoid the disadvantage of labeled LDL (being degraded after internalization). AcLDL was chosen in this test because it has a much quicker blood clearance than LDL, which would enhance the tissue-to-background ratio of radioactivity. Results of this study showed that incorporating  $^{125}\text{I}$ -CI into AcLDL could significantly enhance the selectivity of this compound to atherosclerotic lesions on the aorta of rabbits, and 90% AcLDL was cleared from the blood 30 min postinjection, suggesting that loading radiotracers into AcLDL could be a new approach to detect early atherosclerosis. Two other

radiochemicals, 1,3-dihydroxypropan-2-one 1,3-diiopanoate (DPIP, Figure 3) and cholesteryl 1,3-diiopanoate glyceryl ether (C2I, Figure 4) are undergoing animal studies for their potential as radiotracers for the early detection of atherosclerosis after being incorporated into AcLDL. DPIP has a diglyceride structure, and both DPIP and C2I have six iodines on each molecule, which could provide double the specific radioactivity of the compounds than that of CI after radioiodination.

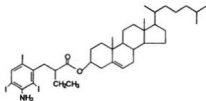


Figure 2. Cholesteryl iopanoate (C1)

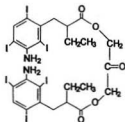


Figure 3. 1,3-dihydroxypropan-2-one 1,3-diiodopanoate (DPIP)

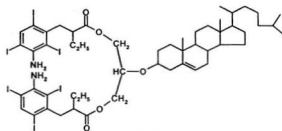


Figure 4. Cholesteryl 1,3-diiodopanoate glyceryl ether (C2I)

**Objectives:**

The first part of this thesis reports on my work on the unhydrolyzable radiochemicals tested in our lab, including C1, DPIP and C2I as the radiotracers and AcLDL as the carriers, for the early detection of atherosclerosis in rabbits. Among the different detecting methods compared above, instrumental approaches provide the easiest and most direct identification of atherosclerotic lesions. However, since instrumental diagnostic methods can identify only the lesions in advanced stages, while early detection of this disease is crucial for the prevention and treatment, radioimaging diagnosis is more preferable. With regard to the radioisotopic imaging techniques, radiolabeled lipoproteins and platelets have shown some clinical potential as imaging agents. But due to poor target-to-background and target-to-blood ratios, these agents are not ideal for imaging coronary or even carotid lesions. Radiolabeled peptides, antibody fragments and metabolic tracers like FDG appear to offer new opportunities for nuclear scintigraphic techniques in the noninvasive imaging of atherosclerosis and atherothrombosis. However, quick degradation and lack of accumulation of these compounds within cells may compromise their advantages. Unhydrolyzable radiochemicals seem to be able to offer significant diagnostic potential after being loaded into chemically modified LDL, in that both the selectivity to and the long-term retention of the radioactivity at the atherosclerotic lesions can be obtained.

The second part of this thesis, entitled "Seal oil markedly enhances the

transfer of a hydrophobic radiopharmaceutical into acetylated low density lipoprotein", describes the techniques we developed in our lab for the purpose of significantly enhancing the incorporation rate of hydrophobic compounds into LDLs. This step is of great importance to the end of using LDLs as carriers to selectively deliver drugs to the target sites. In this part of the studies, four different microemulsions containing DPIP, a potential radioimaging probe, were prepared by means of ultrasonication. The four microemulsions differ in their core lipid component (triolein, canola oil, squalene, or seal oil). The respective DPIP microemulsions were incubated with AcLDL and the amount of DPIP transferred into AcLDL was examined. It was found that the amount of DPIP in the microemulsions expressed as DPIP/oil (w/w) was dependent on the core lipid component of the microemulsion in the order of seal oil ( $0.19 \pm 0.04$ ) > squalene ( $0.15 \pm 0.02$ ) > canola oil ( $0.12 \pm 0.02$ ) > triolein ( $0.07 \pm 0.004$ ). With the exception of canola oil, all microemulsions were found to be effective in enhancing the transfer of DPIP into AcLDL in comparison with commonly used methods, i.e. direct diffusion and detergent solubilization. It was found that DPIP in seal oil resulted in the highest amount of DPIP transferred into AcLDL ( $309.16 \pm 34.82$  vs  $203.19 \pm 64.51$  using squalene and  $151.31 \pm 28.54$  using triolein, DPIP molecules per AcLDL particle).

For the first time, oil isolated from harp seals, a marine mammal that lives in the deep cold North Atlantic ocean, was studied as a major core lipid component of formulating pharmaceutical microemulsions. DPIP in seal oil resulted in the highest amount of DPIP transferred into AcLDL, which is likely due to the highest DPIP

concentration found in this microemulsion as well as the high fluidity of seal oil.

The third part of this thesis, entitled "Incorporation of an  $^{125}\text{I}$ -labeled hexa-iodinated diglyceride analog into low density lipoprotein and high specific uptake by cervical carcinoma cell lines", demonstrates another use of LDLs as carriers of radiotracers: tumor imaging. The feasibility of LDL for cytotoxic drug transport to tumor cells has been explored since the 1980s, when a number of cancer cell lines were found to have higher LDL receptor activity than normal cells. Such differential uptake between tumor cells and normal tissues may provide a unique opportunity to use LDL as a tumor-targeting carrier of radiopharmaceuticals for the clinical management of cancer. In this study, an  $^{125}\text{I}$ -labeled hexa-iodinated diglyceride analog, DPIP, was synthesized and incorporated into LDL using a fusion technique to incorporate approximately 500  $^{125}\text{I}$ -DPIP molecules/LDL particle. Three human cervical tumor cell lines, HeLa, SiHa, and C-33A, were used to examine the binding and LDL receptor-mediated uptake of this  $^{125}\text{I}$ -DPIP-LDL complex. The  $^{125}\text{I}$ -DPIP-LDL conjugate was specifically bound to and taken up by cervical tumor cells through an LDL receptor-mediated endocytotic pathway. The results suggested that this conjugate may be a selective carrier for delivering a hydrophobic radiopharmaceutical to cancers and, particularly, for the diagnosis and therapy of cervical tumors.

Results of all three parts of this thesis indicate that LDL, although not being paid the same attention as a drug carrier these days as 15 years ago, still shows great potential as a drug delivery system.

## **Chapter 2. Acetylated Low Density Lipoprotein as a Carrier to Deliver Radioimaging Probes for the Visualization of Early Atherosclerotic Lesions in Rabbits \***

### **Introduction**

The pathogenesis of atherosclerosis is a long-term process developed in a complex inflammatory and hyperlipidemic environment (Schwartz et al., 1991). It is known that therapeutic and/or dietary intervention is usually successful at an early stage of atherosclerosis. However, angiography, which is the standard method for the detection of arterial obstruction and stenosis, can only identify advanced atherosclerotic lesions which usually require surgical intervention. It has also been suggested that the atherosclerosis is usually more severe than the current diagnostic methodology predicts (Arnett et al., 1979; Vlodaver et al., 1973). Therefore, it is important to develop an early and non-invasive detection method of atherosclerosis to permit a successful therapeutic and dietary intervention.

Although the etiology of atherosclerosis is not fully understood, the involvement of monocytes-macrophages in the arterial intima and their subsequent accumulation of modified LDL have been well elucidated (Gerrity, 1981). Macrophages in the subendothelial space accumulate cholesteryl esters to become

---

\*Published in part in *Pharmaceut. Res.* (see Xiao et al., 1999a).

foam cells (Schwartz et al., 1991; Gerrity, 1981), and foam cells with massive accumulation of cholesteryl esters were observed in atheromatous plaques (Buja et al., 1983). It is known that macrophages express a scavenger receptor for modified LDL such as OxLDL and AcLDL (Goldstein et al., 1979), and that such a receptor was found to be involved in the formation of macrophage foam cell *in vivo* (Yla-Herttuala et al., 1991). The potential for using LDL with its apo B-100 protein radiolabeled, including  $^{125}\text{I}$ -LDL (Sinzinger et al., 1986; Sinzinger and Angelberger, 1988),  $^{125}\text{I}$ -LDL (Roberts et al., 1983),  $^{111}\text{In}$ -LDL (Rosen et al., 1990; Nicolas et al., 1989), and  $^{99\text{m}}\text{Tc}$ -LDL (Lees et al., 1985; Lees et al., 1988; Atsma et al., 1993), as radiomarkers for the detection of atherosclerosis has been investigated. However, when LDL is taken up by the targeted cells, it is quickly degraded by lysosomal enzymes and excreted.

To overcome this problem, we have chosen a cholesteryl ester analogue, Cl, a diglyceride analog, DPIP, and a new compound synthesized in our lab, C2I, as radiotracers. It has been demonstrated that all these three compounds are resistant to hydrolysis *in vivo* (Longino et al., 1983; DeGalan et al., 1988; Xiao et al., 1999a and unpublished data) and thus are able to accumulate in the targeted tissues. In addition, since each LDL particle contains 1,500 cholesteryl ester molecules in its oily core, incorporation of hydrophilic radiotracers can provide more radioactivity than labeling LDL on its apo B-100 protein. Based on the role of macrophages in atherogenesis, we examined the use of AcLDL as a lesion-seeking atherogenic carrier to deliver radiotracers to the site of the early lesions for the purpose of early

diagnosis of atherosclerosis. New Zealand White rabbits were used and early atherosclerotic lesions were induced in several modes. The localizations of the proposed diagnostic probes at the early lesion site were examined and compared.

## **Materials and Methods**

### **Materials**

Thin layer chromatography (TLC) was carried out on silica gel 60, F-254 polyethylene-backed plates (Fisher Scientific) and visualized by UV. Column chromatography was performed on silica gel-60 (230-400 mesh) (Aldrich). High performance liquid chromatography (HPLC) analyses were performed using a Beckman system with a Bondclone 10 C18, 150 X 3.0 mm column (Phenomenex). Radioactivity was measured using a CKB-WALLAC 1277 GAMMAMASTER automatic gamma counter. Sodium dodecyl sulfate polyacrylamide gel electrophoresis (SDS-PAGE) was performed on a Mini-PROTEIN® II Electrophoresis Cell (Bio-Rad). Image analysis was done by BIOQUANT™ System IV.

Carrier-free aqueous Na<sup>125</sup>I was purchased from Mandel Scientific Company Ltd. Pivalic acid was obtained from Aldrich Chemical Co. Canada. Sephadex® G-25 was purchased from Pharmacia Biotech AB, Uppsala, Sweden. Poly-Prep® chromatography columns were obtained from Bio-Rad Laboratories (Hercules, CA). SDS-PAGE molecular weight standards and Bio-Rad protein assay standards were

purchased from Bio-Rad Laboratories (Richmond, CA). L- $\alpha$ -phosphatidylcholine dipalmitoyl (1,2-dihexadecanoyl-*sn*-glycero-3-phosphocholine, DPPC) and DL- $\alpha$ -phosphatidylethanolamine dipalmitoyl (1,2-dihexadecanoyl-*rac*-glycero-3-phosphoethanolamine, DPPE) were purchased from Sigma Chemical Co. Canada. Seal oil was obtained from Terra Nova Fishery, Newfoundland, Canada.

## **Methods**

### *Preparation of AcLDL:*

Fresh human plasma was obtained from the Canadian Red Cross, St. John's, Canada. LDL was isolated as previously described (Schumaker and Puppione, 1986) by the sequential ultracentrifugation of fresh human plasma at 40,000 rpm for 24-40 hours at 8°C using a Beckman L8-M ultracentrifuge and a 60Ti rotor. All LDL preparations were dialysed at 4°C overnight against a buffer containing 0.3 mM EDTA, 150 mM NaCl and 50 mM Tris (pH 7.4). Acetylation of LDL was performed according to a published method (Basu et al., 1976). The AcLDL preparation thus obtained was dialysed at 4°C as described above. Protein concentrations were determined by the Bradford protein assay method with bovine serum albumin (BSA) as the standard (Bradford, 1976).

*Preparation of <sup>125</sup>I-Cl, <sup>125</sup>I-DPIP, and <sup>125</sup>I-C2I:*

Cl and DPIP were synthesized as described (Seevers et al., 1982; Weichert et al., 1986). C2I was novelly synthesized in our lab (Figure 5) as follows:

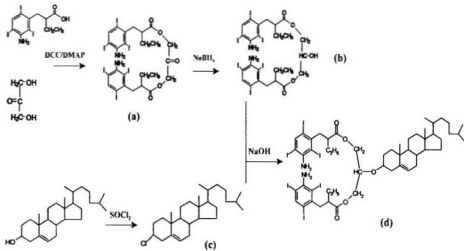
Preparation of DPIP (a) and glyceryl 1,3-diiopanoate (b): Compounds (a) and (b) were synthesized as described (Weichert et al., 1986).

Preparation of cholesteryl chloride (c): cholesterol (5g, 0.0129mol) was added to thionyl chloride (5.5g, 0.046mol, 3.5ml). The mixture was set overnight at 20 °C and then poured into 0.4N sodium hydroxide (about 25ml). The product was extracted three times with ether (1:1), then the combined ether was dried by anhydrous MgSO<sub>4</sub>. Ether was then evaporated to afford a semipure whitish solid, which was further purified by silica gel column chromatography with hexane as the elutant. White cholesteryl chloride solid (3.9 g) was obtained with a yield of 76%.

Preparation of cholesteryl 1,3-diiopanoate glyceryl ether ((d), C2I): cholesteryl chloride (55mg, 0.14mmol) in 2mL of benzene, compound (b) (150mg, 0.125mmol) in 2ml of DMF, and potassium hydroxide (17mg, 0.29mmol) in 2mL of ethanol/water (50:1/v:v) were mixed. The mixture was refluxed overnight, then the solution was concentrated in vacuo at 50 °C and cooled at room temperature. White crystals were generated and purified by column separation (CHCl<sub>3</sub>, silical gel). The yield was about 12.5% (about 25mg). IR(cm<sup>-1</sup>): 3500, 3380(-NH<sub>2</sub>), 2950, 2840(-CH<sub>3</sub>), 1480(C=C), 1740(-C=O), 1380((CH<sub>3</sub>)<sub>2</sub>-CH-), 1600, 920 (Ar). <sup>1</sup>H-NMR(ppm): 8.1(s, 2H, Ar-H), 5.4(s, 1H C=C-H), 4.8(s, 4H, NH<sub>2</sub>), 4.1(m, 4H, CH<sub>2</sub>), 3.7(m, 2H, -O-CH), 3.4-3.2(m, 4H, CH<sub>2</sub>), 2.8(m, 2H, CHCO<sub>2</sub>), 2.2-1.6(m, 22H, CH<sub>2</sub>, CH), 1.1-1.3(m, 10H,

CH<sub>2</sub>), 0.9(d, 15H, CH<sub>3</sub>), 0.7(s, 6H, CH<sub>3</sub>).

Figure 5 Synthesis of cholesteryl 1,3-diopanoate glyceryl ether (C2I)



All three radiotracers were radiolabeled with  $^{125}\text{I}$  via an iodine exchange reaction in a pivalic acid melt (Weichert et al., 1995). The chemical and radiochemical purity of  $^{125}\text{I}$ -CI,  $^{125}\text{I}$ -DPIP, and  $^{125}\text{I}$ -C2I were determined by HPLC and TLC (DeGalan et al., 1986).

*General procedure of incorporation of  $^{125}\text{I}$ -CI,  $^{125}\text{I}$ -DPIP, and  $^{125}\text{I}$ -C2I into AcLDL:*

A mixture of 12 mg DPPC, 8 mg DPPE, 20 mg seal oil and 1 mg radiolabeled drug in chloroform was dried with a gentle stream of nitrogen, and re-suspended in 10 mL of saline. The suspension was sonicated for 2 hours using a Virosonic Cell disrupter Model 16-850 at 40-50 watts at about  $-10\text{ }^{\circ}\text{C}$ . The mixture was then centrifuged at 40,000 rpm for 20 hours at  $4\text{ }^{\circ}\text{C}$  in a Beckman SW41 rotor. The microemulsion that floated to the top of the centrifuge tube was collected. Microemulsion thus obtained was incubated with AcLDL at  $37\text{ }^{\circ}\text{C}$  for 24 hours. The resultant mixture was centrifuged again to obtain  $^{125}\text{I}$ -CI/AcLDL.

*Characterization of  $^{125}\text{I}$ -CI/AcLDL:*

*Column chromatography:* After separation from microemulsion by ultracentrifugation,  $^{125}\text{I}$ -CI/AcLDL (about 2 mg/mL), 500 mL, was loaded onto a Poly-Prep<sup>®</sup> chromatography column packed with about 1g of Sephadex<sup>®</sup> G-25 and eluted with phosphate buffered saline (PBS pH = 7.4). Fractions of 0.5 mL each were collected. The radioactivity and protein content associated with each fraction were determined and plotted.

*Electrophoresis:* In order to assess the integrity of the apo B-100 protein associated with  $^{125}\text{I}$ -CI/AcLDL, the  $^{125}\text{I}$ -CI/AcLDL sample was examined by SDS-PAGE and compared with native LDL and AcLDL as reported (Cardin et al., 1986).

*Stability of  $^{125}\text{I}$ -CI/AcLDL in plasma:*  $^{125}\text{I}$ -CI/AcLDL was incubated with plasma according to a reported method (Smadi-Baboli et al., 1993) with modifications.  $^{125}\text{I}$ -CI/AcLDL, 1mL, was incubated with 5 mL of human plasma at 37 °C for 24 hours. Different fractions including very low density lipoprotein (VLDL), LDL, high density lipoprotein (HDL), and lipoprotein deficient serum (LPDS) were separated as previously described (Schumaker and Puppione, 1986). The radioactivity in each fraction was determined.

*Animal model and protocol for  $^{125}\text{I}$ -CI/AcLDL:*

Eight female New Zealand White rabbits (3.20–4.75 kg) were randomly divided into two groups. One group was maintained on normal rabbit chow (n=4) and the other group on rabbit chow supplemented with 1% cholesterol and 2% lard (n=4) for 6 weeks to induce the development of early stage atherosclerotic lesions. The  $^{125}\text{I}$ -CI/AcLDL preparation was then injected via the marginal ear vein to both control and atherosclerotic lesion rabbits at 2  $\mu\text{Ci}/\text{kg}$ . Blood samples were taken at 5 minutes, 30 minutes, 1 hour, 2 hours, 4 hours, 8 hours, 24 hours, 48 hours and 72 hours after injection. The rabbits were then sacrificed and 4% formaldehyde buffer was infused into the heart to fix the organs. Tissues, including aorta, liver, spleen, lung, kidney and heart, were removed for determination of radioactivity using a gamma counter.

The aortae that were free of fat and connective tissues were opened longitudinally, and fixed in 4% formaldehyde for 48 hours. After fixation, the aortae were stained with Sudan IV solution, and subsequently exposed to Kodak X-OMAT™ AR film and stored in Kodak X-Omatic cassettes at -70 °C for one week.

*Animal model and protocol for <sup>125</sup>I-DPIP/AcLDL:*

Nine male New Zealand White rabbits (3.2 kg - 4.1 kg) were divided into two groups randomly. Both groups were fed with 1% cholesterol diet for 3 weeks. Then surgery was performed to induce carotid artery injuries. The 1% cholesterol diet was maintained for both groups for a further 6 weeks, and in the meantime, an anti-atherogenic agent was applied to one group (n=5) at 10 mg/kg/day. Rabbits were injected with 2 µCi/kg <sup>125</sup>I-DPIP 24 hours prior to sacrifice. Tissues including liver, spleen, lung, kidney, adrenal gland, blood, and aorta were separated and counted. Autoradiogram was performed on the aortae of both groups as described above.

*Animal model and protocol for <sup>125</sup>I-C2I/AcLDL:*

Ten male New Zealand White rabbits (2.5 kg-4.7 kg) were randomly divided into three groups. One group was maintained on normal rabbit chow (n=4, control group) for twelve weeks, one group on rabbit chow supplemented with 1% cholesterol (n=4, cholesterol group) for 12 weeks to induce the development of early stage atherosclerotic lesions, and the other group was treated the same as cholesterol group except for being fed with the anti-atherogenic agent (10mg/kg/day)

simultaneously (n=2, anti-atherogenic agent group). The <sup>125</sup>I-C2I/microemulsion/AcLDL preparation was then injected via the marginal ear vein to all the three groups of rabbits at a dose of 15 µ Ci/kg. Twenty four hours postinjection the rabbits were sacrificed and tissues, including liver, spleen, lung, kidney adrenal gland, blood and aortae, were sampled for determination of radioactivity using a gamma counter. Results of biodistribution were shown in Figure 9 and Table IV.

#### *In vivo stability tests of DPIP and C2I*

*In vivo* stability tests were performed according to a published method (DeGalan et al., 1988). Briefly, 10 g liver was homogenized with a Brinkmann homogenizer (model PT 10/35) for 3 minutes. The homogenate was then extracted twice by 90 mL CHCl<sub>3</sub>:CH<sub>3</sub>OH (2:1/v:v). The extract was filtered and evaporated. The residue was then analyzed by TLC with CHCl<sub>3</sub>:CH<sub>3</sub>OH (25:2 /v:v) as the development solution. The plates was cut into ten 0.5cm pieces. The stability was expressed as the proportion of the radioactivity associated with the DPIP or C2I spot out of the total radioactivity of the ten pieces.

## **Results and Discussion**

It is clear that macrophages play an important role in the formation of atherosclerotic lesions (via the formation of the foam cells) (Schwartz et al., 1991;

Gernity, 1981; Buja et al., 1983; Yla-Herttuala et al., 1991) and they express scavenger receptors that mediate the uptake of AcLDL. It is believed that CI incorporated into AcLDL (CI/AcLDL) is taken up by macrophages (Kenji et al., 1988) through the scavenger receptor pathway. We have, therefore, examined the potential of using AcLDL to deliver radiotracers, such as CI, DPIP and C2I, to early atherosclerotic lesions induced in rabbits. These radiotracers can be easily labeled with  $^{131}\text{I}$  or  $^{125}\text{I}$ , and will allow the visualization of the lesions using gamma scintigraphy technology if the proposed method can selectively target these tracers to the lesion sites.

#### *Preparation of $^{125}\text{I}$ -CI/AcLDL*

$^{125}\text{I}$ -CI was synthesized and its radiochemical purity was found to be more than 96%. Microemulsions have been widely employed in loading drugs into LDL, and in our studies, seal oil was novelly used to form microemulsion for its high efficiency of transferring the drugs to LDL (Xiao et al., 1999b), presumably because seal oil contains high levels of highly unsaturated triglycerides, which may allow for high solvation of hydrophobic drugs and the increase of fluidity. With the loading method we employed, up to five hundred  $^{125}\text{I}$ -CI molecules can be incorporated into each AcLDL particle (Xiao et al., 1999a). The specific radioactivity of the  $^{125}\text{I}$ -CI/AcLDL was about 2.5  $\mu\text{Ci/mL}$ .

#### *Characterization of $^{125}\text{I}$ -CI/AcLDL*

## NOTE TO USERS

Page(s) not included in the original manuscript and are unavailable from the author or university. The manuscript was scanned as received.

This reproduction is the best copy available.

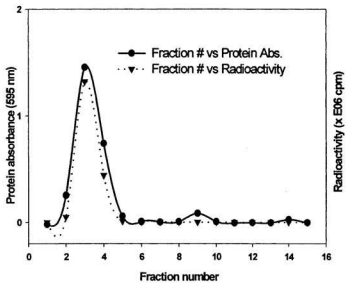


Figure 6. Chromatograms of gel filtration of  $^{125}\text{I}$ -CI/AcLDL preparation with respect to its radioactivity ( $\blacktriangledown$ ) and protein concentration ( $\bullet$ ).

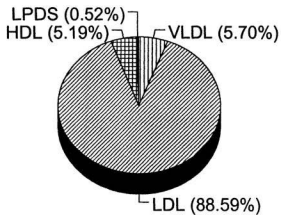


Figure. 7 Distribution of radioactivity upon incubation of  $^{125}\text{I}\text{-Cl/AcLDL}$  with plasma. Values are the % of initial radioactivity associated with individual fractions after incubation.

*Analysis of animal data for  $^{125}\text{I}$ -CI/AcLDL imaging*

Although there are many published methods on generating atherosclerotic lesions in rabbits (Roberts et al., 1983; Atsma et al., 1993; Narula et al., 1997; Allison et al., 1997), early atherosclerosis was induced in New Zealand White rabbits in this case by feeding a regular diet supplemented with 1% cholesterol and 2% lard for six weeks while the control group was maintained on a regular diet. Cholesterol, triglyceride, HDL, and LDL levels in blood were measured in both control and atherosclerotic groups. The results are summarized in Table II. The atherosclerotic group demonstrated increased levels of all lipids measured.  $^{125}\text{I}$ -CI/AcLDL was then given intravenously to both control and atherosclerotic groups at 2  $\mu\text{Ci}/\text{kg}$ . The radioactivity in blood samples taken at different time intervals was measured. The results presented in Figure 8 and Table III demonstrated that the clearance of  $^{125}\text{I}$ -CI/AcLDL from blood follows a two compartment model with  $t_{1/2\alpha}$  of 0.28 hr and 1.09 hr and  $t_{1/2\beta}$  of 56.60 hr and 43.79 hr for atherosclerotic and control groups, respectively. The difference in  $t_{1/2}$  values between two the groups was not significant ( $p>0.05$ ).

Table II. Comparison between atherosclerotic and control rabbits of cholesterol, triglyceride, HDL and LDL contents in blood. (Average  $\pm$  SD)

	Atherosclerotic group	Control group
Cholesterol (mmol/L)	60.01 $\pm$ 8.79	0.57 $\pm$ 0.12
Triglyceride (mmol/L)	4.90 $\pm$ 2.67	0.69 $\pm$ 0.04
HDL (mmol/L)	18.65 $\pm$ 3.00	0.37 $\pm$ 0.01
LDL (mmol/L)	39.13 $\pm$ 4.57	0.16 $\pm$ 0.08

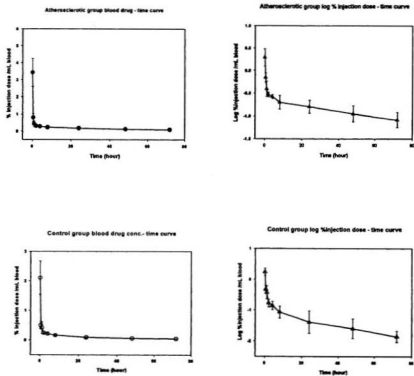


Figure. 8 Amount of  $^{125}\text{I}\text{-Cl}$  in blood versus time after i.v. injection of  $^{125}\text{I}\text{-Cl}$  at 2  $\mu\text{Ci}/\text{kg}$  in atherosclerotic ( $\bullet, \blacktriangle$ ) and control rabbits ( $\circ, \triangle$ ).  $n=4$ .

Table III. Pharmacokinetic parameters of the radioactivity in the blood of atherosclerotic and control rabbits after i.v. injection of  $^{125}\text{I}$ -Cl/AcLDL at 2  $\mu\text{Ci/kg}$  dose. (Average  $\pm$  SD)

	$k_d(\text{hr}^{-1})$	$t_{1/2}(\text{hr})$	$k_e(\text{hr}^{-1})$	$t_{1/2}(\text{hr})$	$V(\text{mL}\cdot\text{kg}^{-1})$	$\text{CL}(\text{mL}\cdot\text{kg}^{-1}\cdot\text{hr}^{-1})$
Atherosclerotic group	$2.59 \pm 0.50$	$0.29 \pm 0.054$	$0.012 \pm 0.0014$	$56.60 \pm 6.99$	49.2	128.04
Control group	$0.70 \pm 0.23$	$1.09 \pm 0.44$	$0.16 \pm 0.0028$	$43.79 \pm 8.59$	144.23	102.8

$k_d, k_e$ : elimination constant

$t_{1/2}$ : drug half life in blood

V: Volume of distribution

CL: Clearance

The tissue distribution studies suggested that there were no significant differences between the atherosclerotic group and control group in all tissues with exception of the aorta and blood at 72 hours. The radioactivity in both aorta and blood expressed as percent of injected dose per gram of organ, was about 8 times higher for the lesion group than for the control group (Figure 9 and Table IV). The increased radioactivity level in the aorta of atherosclerotic rabbits was likely due to the higher level of scavenger receptor which mediates the uptake of AcLDL in the lesion sites. The higher levels of  $^{125}\text{I}$ -Cl in blood for this group of animals can be explained by their higher blood cholesterol levels (Table II). From Figure 10, it was found that the lesion areas which correlated with the autoradiography was about 5% of the total aorta. The specific radioactivity of the lesions of aorta was the highest among all the tissues taken, including liver and spleen (Table IV). Thus, we have shown that using AcLDL as a targeting carrier to atherosclerotic plaques achieves a high accumulation of  $^{125}\text{I}$ -Cl at these sites, as shown by the presence of the most radioactive spots in the lesioned areas among the major organs examined.

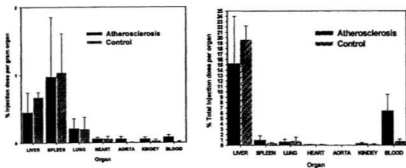


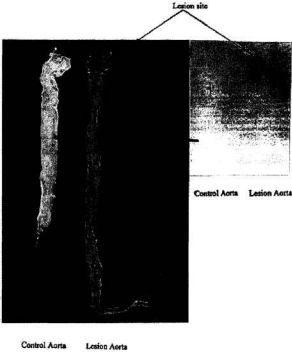
Figure 9. Distribution of radioactivity in various tissues expressed as % of administered dose/g tissue (left) or % of administered dose/whole tissue (right) in atherosclerotic and control rabbits after i.v. injection of  $^{125}\text{I}\text{-Cl/AcLDL}$  at  $2\ \mu\text{Ci/kg}$ .

Table IV. Comparison between atherosclerotic and control rabbits of distribution of radioactivity in various tissues after i.v. injection of  $^{125}\text{I}$ -Cl/AcLDL at 2  $\mu\text{Ci/kg}$ . (Average  $\pm$  SD)

Tissue	Atherosclerotic group (n=4) % administered dose/g tissue	Control group (n=4) % administered dose/g tissue
LIVER	0.46 $\pm$ 0.29	0.68 $\pm$ 0.068
SPLEEN	0.98 $\pm$ 0.87	1.04 $\pm$ 0.57
LUNG	0.21 $\pm$ 0.14	0.20 $\pm$ 0.17
HEART	0.060 $\pm$ 0.017	0.062 $\pm$ 0.032
<b>AORTA</b>	<b>0.056 <math>\pm</math> 0.034<sup>a</sup></b>	<b>0.0069 <math>\pm</math> 0.0019</b>
KIDNEY	0.057 $\pm$ 0.022	0.032 $\pm$ 0.017
<b>BLOOD</b>	<b>0.087 <math>\pm</math> 0.030<sup>a</sup></b>	<b>0.013 <math>\pm</math> 0.0073</b>

<sup>a</sup>p < 0.05

Figure 10. Correlation of Sudan IV staining (left) and autoradiography (right) - CI.



Sudan IV staining was carried out on the aortae in order to visualize the atherosclerotic lesions. The red lipid stain is an indication of lipid-laden foam cells, a hallmark of early atherosclerosis. As shown in Figure 10, the lesion area corresponded to about 5% of the whole aorta. The most severe lesion region was the ascending aorta at the aortic arch. Blood flow through this section of aorta is turbulent due to the curve of the aortic arch and the three large branches. The highest incidence of human atherosclerosis is to be found in this region of the aorta. The hottest spots detected in the aortae of lesioned rabbits were strongly correlated to the location of highest incidence of human atherosclerosis.

Autoradiographs of aortae removed from both normal and atherosclerotic rabbits are shown in Figure 10. The image was the result of the accumulation of  $^{125}\text{I}$ -Cl/AcLDL. The area of the image superimposed with the staining result, suggesting  $^{125}\text{I}$ -Cl/AcLDL has been taken up by the lesion. Both Sudan IV and autoradiography showed negative results with the aorta from control rabbits.

*Results of using  $^{125}\text{I}$ -DPIP/AcLDL complex as the radiotracer*

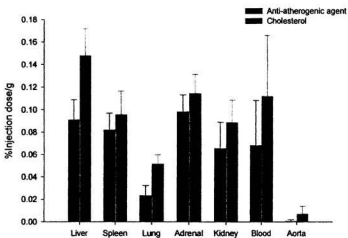
$^{125}\text{I}$ -DPIP was selected as an alternative to  $^{125}\text{I}$ -Cl because each DPIP molecule has two benzene rings, and each of its benzene rings carries three iodines. Since about same amount of DPIP was incorporated into AcLDL as Cl (unpublished data), DPIP has the potential of bearing 6 radiolabeled iodines and having higher specific radioactivity than Cl, which presumably makes it a more attractive candidate for the purpose of this study. Extraction of DPIP from livers of rabbits showed that

87% of the radioactivity was associated with DPIP, indicating that DPIP is chemically stable *in vivo* (unpublished data). However, according to our animal test with  $^{125}\text{I}$ -DPIP/AcLDL, although a difference between the drug tissue distribution of the anti-atherogenic agent treated group and cholesterol diet group was observed (Table V and Figure 11), indicating that the anti-atherogenic agent could alleviate the procedure of atherosclerosis in rabbits, the autoradiograms were not clearly showing any difference between the lesions suggested by Sudan IV staining (data not shown). In addition, compared with  $^{125}\text{I}$ -Cl, less  $^{125}\text{I}$ -DPIP was found in all rabbit tissues even though the administered radioactivity for  $^{125}\text{I}$ -DPIP and  $^{125}\text{I}$ -Cl were the same, and the observation time was shorter (1 day for  $^{125}\text{I}$ -DPIP and 3 days for  $^{125}\text{I}$ -Cl). A possible explanation to this is that DPIP, compared with Cl, has a much smaller molecular structure, and a higher hydrophilicity. Therefore, higher levels of  $^{125}\text{I}$ -DPIP may have been excreted through the renal clearance system.

Table V. Comparison between atherosclerotic and control rabbits of distribution of radioactivity in various tissues after i.v. injection of  $^{125}\text{I}$ -DPIP/AcLDL at 2  $\mu\text{Ci/kg}$ . (Average  $\pm$  SD)

Tissue	Anti-atherogenic agent treated group (n=5) % administered dose/g tissue	Cholesterol diet group (n=4) % administered dose/g tissue
Liver	0.091 $\pm$ 0.018	0.15 $\pm$ 0.024
Spleen	0.082 $\pm$ 0.015	0.096 $\pm$ 0.021
Lung	0.023 $\pm$ 8.7x10 <sup>-3</sup>	0.052 $\pm$ 8.1x10 <sup>-3</sup>
Adrenal	0.098 $\pm$ 0.015	0.11 $\pm$ 0.017
Kidney	0.065 $\pm$ 0.024	0.089 $\pm$ 0.020
Blood	0.068 $\pm$ 0.040	0.11 $\pm$ 0.054
Aorta	0.00069 $\pm$ 0.00012	0.0073 $\pm$ 0.0066

Figure 11. Distribution of radioactivity in various tissues expressed as % of administered dose/g tissue in atherosclerotic and control rabbits after i.v. injection of  $^{125}\text{I}$ -DPIP/AcLDL at  $2\ \mu\text{Ci/kg}$ .



### *Results of using <sup>125</sup>I-C2I/AcLDL complex as the radiotracer*

To combine the advantages of CI and DPIP, and overcome the drawback of DPIP, we have designed and synthesized a new compound, C2I. C2I combines the structure of DPIP, which provides six iodines for radiolabeling (twice of those on CI), and a backbone of cholesterol, which enhances the hydrophobicity of the compound, so as to avoid the renal clearance of the drug (Figures 2-4). In the molecule of C2I, the cholesteryl part and the diglyceride part are linked via an ether bond, which is resistant to the hydrolysis by lysosomal enzymes in cells. Therefore, the compound is expected to be stable in the cytoplasm and subcellular compartments. *In vivo* stability test showed that 91.2% of the radioactivity in liver cells was still associated with C2I (see Materials and methods), indicating that C2I is chemically stable *in vivo*.

It was found that there was no statistical difference between the anti-atherogenic agent treated group and cholesterol fed group in terms of the localizations of <sup>125</sup>I-C2I in liver, spleen, lung, kidney, adrenal gland, blood and aorta, indicating that the anti-atherogenic agent had no effect on the distribution of <sup>125</sup>I-C2I in rabbits within 24 hours (Figure 12, Table VI). While the localizations of <sup>125</sup>I-C2I in adrenal gland for both the anti-atherogenic agent and the cholesterol group were significantly lower than that in control rabbits ( $p < 0.05$ ), and the distributions of <sup>125</sup>I-C2I in blood and aortae of the anti-atherogenic agent and cholesterol group were significantly higher than those for control group (2 to 4 times, Figure 12 and Table VI). In autoradiography studies, lesions were clearly shown and in correlation with the Sudan IV staining results, and the places without lesion did not show any image

on the film, indicating that  $^{125}\text{I}$ -C2I was selectively located at the aortic plaques (Figure 13).

Figure 12. Biodistribution of  $^{125}\text{I}$ -C2I in the anti-atherogenic agent group, cholesterol group, and control group rabbits.

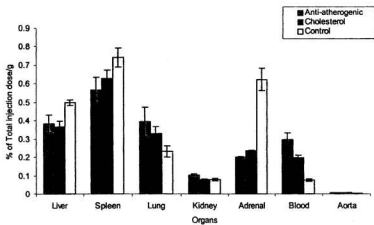


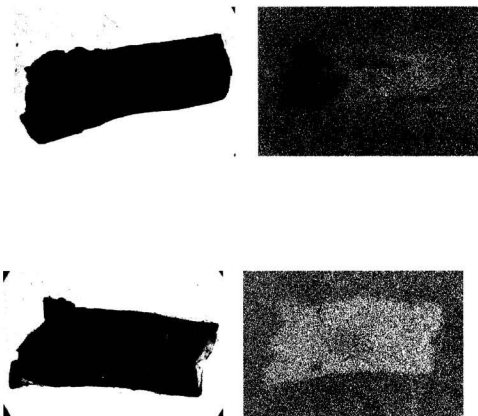
Table VI. Comparison between atherosclerotic and control rabbits of distribution of radioactivity in various tissues after i.v. injection of  $^{125}\text{I}$ -C2I at 15  $\mu\text{Ci/kg}$  in the anti-atherogenic agent group, cholesterol group, and control group rabbits (Average  $\pm$  SD).

	Anti-atherogenic agent group (Aa) % administered dose/g tissue	Cholesterol group (Ch) % administered dose/g tissue	Control group (Co) % administered dose/g tissue
Liver	0.38 $\pm$ 0.097	0.37 $\pm$ 0.061	0.50 $\pm$ 0.030
Spleen	0.57 $\pm$ 0.13	0.63 $\pm$ 0.090	0.74 $\pm$ 0.10
Lung	0.39 $\pm$ 0.16	0.33 $\pm$ 0.075	0.23 $\pm$ 0.060
Kidney	0.10 $\pm$ 0.012	0.077 $\pm$ 0.0090	0.079 $\pm$ 0.014
Adrenal Gland	0.20 $\pm$ 0.012	0.23 $\pm$ 0.0091	0.62 $\pm$ 0.12
Blood	0.30 $\pm$ 0.076*	0.20 $\pm$ 0.029*	0.074 $\pm$ 0.015
Aorta	0.0065 $\pm$ 0.0039*	0.0070 $\pm$ 0.0012*	0.0033 $\pm$ 0.00067

\* Significant difference compared with controls,  $p < 0.05$

Figure 13. Correlation of Sudan IV staining (left) and autoradiography (right) - C2I.  
Lesion Aorta

Control Aorta



## Conclusion

Our studies demonstrated that selective uptake and retention of  $^{125}\text{I}$ -CI at the site of early atherosclerotic lesions can be achieved via the use of AcLDL as the carrier. This finding warrants further animal studies.  $^{125}\text{I}$ -DPIP also revealed differences between the drug distributions of two rabbit groups with different degrees of atherosclerosis. However, because of its high hydrophilicity, the high specific radioactivity of DPIP may be compromised by its quick renal clearance.  $^{125}\text{I}$ -C2I is promising as a new radiotracer compound for the early diagnosis of atherosclerosis. Its advantages are its higher specific radioactivity, compared to  $^{125}\text{I}$  CI, and higher hydrophobicity, compared to  $^{125}\text{I}$ -DPIP. Further studies will be concentrated on replacing  $^{125}\text{I}$  with  $^{131}\text{I}$  or  $^{123}\text{I}$  in  $^{125}\text{I}$ -CI or  $^{125}\text{I}$ -C2I to acquire imaging pictures of rabbits extracorporeally using gamma scintigraphy.

## NOTE TO USERS

Page(s) not included in the original manuscript and are unavailable from the author or university. The manuscript was scanned as received.

57

This reproduction is the best copy available.

**UMI**<sup>®</sup>

LDL or AcLDL particles (Samadi-Baboli et al., 1990; Vitols et al., 1990; Liu and Liu, 1995). In this chapter, we report on the transfer of DPIP into AcLDL via the preparation of DPIP microemulsions using triolein, canola oil, squalene, and seal oil as the core lipid component. The amount of DPIP transferred from the microemulsions to AcLDL was determined and compared. For the first time, seal oil was used to formulate microemulsions. The harp seal, a marine mammal, lives in an extremely cold environment (-40 to -70 °C). In such a cold condition, its circulatory system can still function well and its hydrophobic lipids such as triglycerides, cholesterol and cholesteryl esters remain in liquid state but not crystallized. Although little research has been done to explain this fascinating phenomenon, it has been speculated that the unique polyunsaturated long chain fatty acids found in seal oil may contribute to greater fluidity of hydrophobic compounds in harp seals at the extremely low temperatures. In addition, seal oil has strong anti-oxidant properties which are useful in formulating stable microemulsions.

## **Materials and Methods**

### **Materials**

TLC was carried out on Fisher Scientific silica gel 60, F-254 polyethylene-backed plates and visualized by UV. HPLC analyses were performed using a

Beckman system with a Phenomenex Bondclone 10C18, 150 X 3.0 mm column. Radioactivity was measured using a CKB-WALLAC 1277 GAMMAMASTER automatic gamma counter. SDS-PAGE was performed on a BIO-RAD Mini-PROTEIN® II Electrophoresis Cell. A Philips EM 300 was used for electron microscopy (EM) and particles were negatively stained with 1% uranyl acetate. Image analysis was done by BIOQUANT™ System IV.

Carrier-free aqueous solutions of Na<sup>125</sup>I were purchased from DuPont NEN Research Products (Boston, MA). Pivalic acid was obtained from Aldrich Chemical Co. Canada. Sephadex® G-25 was purchased from Pharmacia Biotech AB, Uppsala, Sweden. Poly-Prep® chromatography columns were obtained from Bio-Rad Laboratories (Hercules, CA). SDS-PAGE molecular weight standards and Bio-Rad protein assay kits were purchased from Bio-Rad Laboratories (Richmond, CA). DPPC, DPPE, and squalene were purchased from Sigma-Aldrich Canada. Canola oil was purchased from a local supermarket. Seal oil from harp seal, *Phoca groenlandica*, was obtained from Terra Nova Fishery Ltd., Newfoundland, Canada.

## **Methods**

### *Preparation of DPIP and <sup>125</sup>I-DPIP*

DPIP was synthesized as reported (Weichert et al., 1986) and radiolabelled with <sup>125</sup>I via an isotope exchange reaction in a pivalic acid melt (DeGalan et al., 1988). The chemical and radiochemical purity of <sup>125</sup>I-DPIP were determined by

HPLC and TLC as described before (DeGalan et al., 1988).

#### *Preparation of DPIP microemulsions*

DPIP microemulsions were prepared using triolein, canola oil, squalene, and seal oil, respectively, as the core lipid component. DPPC (12 mg), DPPE (8 mg), triolein, canola oil, squalene, or seal oil (20 mg), DPIP(10 mg) and  $^{125}\text{I}$ -DPIP(0.05 mg) were dissolved in chloroform, dried with a gentle stream of nitrogen, and suspended in 10 mL of saline at 25°C.  $^{125}\text{I}$ -DPIP was used as a radioactive tracer for analysis. The suspension was sonicated for 2 hours with a Virosonic Cell Disrupter Model 16-850 at 40-50 watts while being cooled in a -10 °C salt-ice-water bath under a nitrogen stream. The mixture was then centrifuged at 40,000 rpm for 20 hours at 4 °C using a Beckman SW41 rotor and a Beckman L5-65 ultracentrifuge. The microemulsion which floated to the top of the centrifuge tubes was collected, and subjected to EM and image analysis. The amount of DPIP in the individual microemulsions was determined using a CKB-WALLAC 1277 GAMMAMASTER automatic gamma counter.

#### *Preparation of AcLDL*

Fresh human plasma was obtained from the Canadian Red Cross Society, St. John's, Newfoundland, Canada. LDL was isolated as previously described (Schumaker and Puppione, 1986) by sequential ultracentrifugation of fresh human plasma at 40,000 rpm for 24-40 hours at 8 °C using a Beckman L8-M ultracentrifuge

and a 60Ti rotor. LDL was dialysed at 4 °C overnight against a buffer containing 0.3 mM EDTA, 150 mM NaCl and 50 mM Tris (pH 7.4). Protein concentrations were determined by the method of Bradford (Bradford, 1976). Acetylation of LDL was performed as described by Basu and Goldstein (Basu et al., 1976). AcLDL was dialysed and protein concentrations were determined.

#### *Incorporation of DPIP into AcLDL*

The <sup>125</sup>I-DPIP microemulsions were incubated with AcLDL at 37 °C for 24 hours at a molar ratio of DPIP to AcLDL of 1000:1. AcLDL loaded with <sup>125</sup>I-DPIP (<sup>125</sup>I-DPIP/AcLDL) was then separated from microemulsions by ultracentrifugation as described (Schumaker and Puppione, 1986). The DPIP content in <sup>125</sup>I-DPIP/AcLDL was determined by  $\gamma$ -counting.

DPIP was also incorporated into AcLDL using direct diffusion (Shaw et al., 1988) and detergent solubilization (DeForge et al., 1992) with minor modifications. In brief, for the method of direct diffusion, DPIP was dissolved in chloroform in a glass vial and dried under a stream of nitrogen to form a thin film on the wall of the vial. AcLDL was added to the vial and incubated at 37 °C for 24 hours. For the method of detergent solubilization, DPIP was dissolved in saline in the presence of Tween 20 (<3%), and incubated with AcLDL at 37 °C for 24 hours. The molar ratio of DPIP to AcLDL used remained the same as above.

#### *Characterization of <sup>125</sup>I-DPIP/AcLDL*

<sup>125</sup>I-DPIP/AcLDL (500 mL), about 1 mg/mL, was loaded onto 1g of Sephadex® G-25 in a Poly-Prep® chromatography column and eluted with phosphate buffered saline (PBS pH 7.4). Fractions of 0.5 mL were collected, and radioactivity and protein content of each fraction were measured and plotted.

In order to assess the integrity of the apo B-100 protein of <sup>125</sup>I-DPIP/AcLDL, samples were analyzed by SDS-PAGE and electron microscopy (EM) as described (DeForge et al., 1992).

## **Results and Discussion**

Our previous studies suggested that AcLDL could be used as a carrier to deliver radiolabelled CI, a cholesterol ester analog, to atherosclerotic lesions in rabbits (Xiao et al., 1999). Compared to CI, DPIP is considered to be a better probe for the detection of atherosclerotic lesions. Through radio-iodination, the six iodine atoms on each DPIP molecule provide higher specific radioactivity than CI. This is desirable for the accumulation of the high radioactivity required for diagnostic purposes. In this report, the loading of DPIP into AcLDL was studied.

The methods of direct diffusion and detergent solubilization have been widely used for loading lipophilic drugs into LDL or AcLDL due to their simplicity (Firestones, 1994). Microemulsions have also been employed to transfer various drugs into LDL or AcLDL (Samadi-Baboli et al.,1990; Vitols et al.,1990; Liu and Liu,1995; Sqalli-Houssaini et al.,1994), and so far triolein has been one of the most commonly used core lipid components. In this study, squalene and seal oil were used as the core

lipid components of microemulsions for the first time. Squalene, a highly unsaturated hydrocarbon ( $C_{30}H_{50}$ ) that is an intermediate product in the synthesis of cholesterol, was shown to be capable of re-supplying cells with much needed oxygen. In recent years, seal oil has been of interest for its potential use in the maintenance of human health (Simopoulos, 1991; Christensen et al., 1994; Osterud et al., 1995; Christensen and Hoy, 1996). The  $\omega$ -3 polyunsaturated long chain fatty acids found in seal oil have been shown to be beneficial in lowering blood pressure (Bonna et al., 1990), reducing triacylglycerols (Harris et al., 23), and modulating cell function and cell reactivity to external stimuli (Fox and Dicorleto, 1988). In addition, seal oil appears to be very resistant to oxidation, which is desirable for preparation of stable microemulsions.

The preparation of the microemulsions was carried out by hydrating a dried film of the lipid mixtures with saline at room temperature. This was followed by ultrasonication, during which the aqueous dispersions were cooled in a salt-ice bath at  $-10^{\circ}\text{C}$  to prevent overheating due to the sonication. It is possible that the preparation of the microemulsions at a temperature below the gel-liquid crystalline phase transition temperature of the phospholipids would result in limited hydration of the phospholipids. However, the electron micrographs show structures that are typical of those observed in preparations of microemulsions formed by sonication at temperatures above the phospholipid transition temperatures (Redgrave and Maranhao, 1985). Furthermore, these authors reported that the microemulsion particles were 50-200nm in diameter. This compares well with our preparations that

have diameters of 30-90nm (Figure 15). The slightly larger diameter seen by Redgrave and Maranhao could be due to the use of a phosphatidylcholine species containing unsaturated fatty acids that increase the molecular area of the phospholipid compared with the fully saturated phosphatidylcholines that were used in our preparations.

The concentrations of DPIP in microemulsions with triolein, canola oil, squalene and seal oil as the core lipid component were compared. It was found that the amount of DPIP eventually loaded into the microemulsions expressed as DPIP/oil (w/w) was in the order of seal oil ( $0.19 \pm 0.04$ ) > squalene ( $0.15 \pm 0.02$ ) > canola oil ( $0.12 \pm 0.02$ ) > triolein ( $0.07 \pm 0.004$ ) as shown in Figure 14. EM (Figure 15) and image analysis (Figure 16) results showed that the size of the microemulsion particles is in the same order of seal oil (longest diameter =  $67.8 \pm 25.37$  nm) > squalene (longest diameter =  $58.2 \pm 22.01$  nm) > canola oil (longest diameter =  $52.9 \pm 16.05$  nm) > triolein (longest diameter =  $40.6 \pm 13.5$  nm).

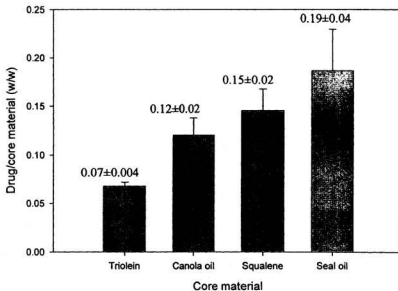


Figure 14. Comparison of DPIP concentrations in microemulsions using triolein, canola oil, squalene and seal oil, respectively, as the core lipid component. The results are expressed as the ratio of DPIP to oil (w/w).

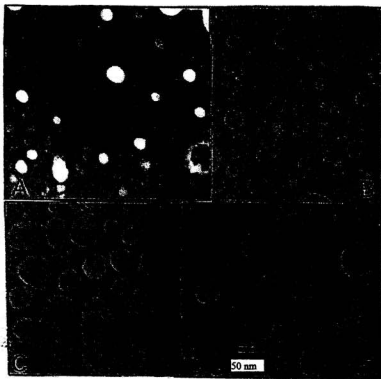


Figure 15. Electron micrographs of DPIP microemulsions using triolein (A), canola oil (B), squalene (C) and seal oil (D), respectively, as the core lipid component. All panels are shown at the same magnification.

Figure 16. Image analysis of DPIP microemulsions using triolein, canola oil, squalene, and seal oil, respectively, as the core lipid component. The left four panels are the distributions of image areas of four microemulsions ( $\text{nm}^2$ ) and the right four panels are the distributions of longest diameters of the four microemulsions (nm). See next page.

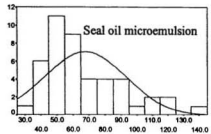
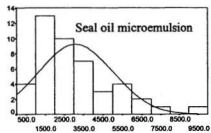
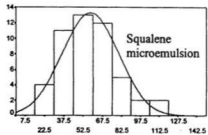
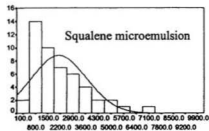
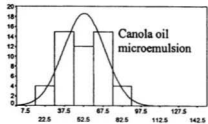
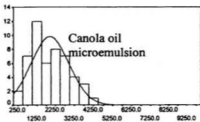
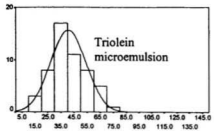
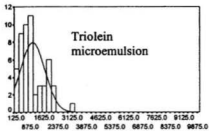
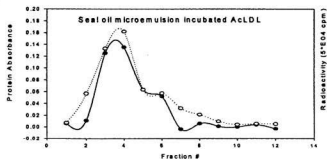
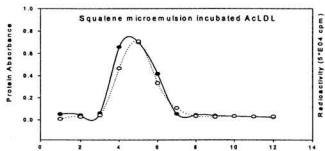
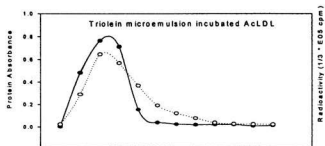


Image area of microemulsions (nm<sup>2</sup>)

Longest diameter of microemulsions (nm)

Upon incubation of the DPIP microemulsions with AcLDL, DPIP was successfully transferred into AcLDL, with the exception of the canola oil microemulsion, in which AcLDL was found to be aggregated (data not shown). DPIP/AcLDL preparations were subjected to gel filtration. The chromatograms of radioactivity and protein contents were plotted. As shown in Figure 17, radioactivity (due to  $^{125}\text{I}$ -DPIP) and protein content were superimposed, suggesting that DPIP was transferred to AcLDL (or DPIP/AcLDL formed). SDS-PAGE results of DPIP/AcLDL indicated that the integrity of apo B-100 protein was intact in comparison with native LDL and AcLDL (data not shown). The poor results obtained with canola oil are possibly due to the presence of preservatives or other additives in the commercial canola oil.

Figure 17. Confirmation of  $^{125}\text{I}$ -DPIP incorporation into AcLDL particles using three different lipid microemulsions (top panel: triolein; middle panel: squalene; and bottom panel: seal oil).  $^{125}\text{I}$ -DPIP/AcLDL conjugates were analyzed by gel filtration chromatography through Sephadex G-25 with PBS. The radioactivity and protein content of each fraction were determined as described in the section of Materials and Methods. See next page.



The transfer efficiency of DPIP from the triolein, squalene, and seal oil microemulsions to AcLDL was also compared with that of two commonly used methods, i.e., direct diffusion and detergent solubilization. As shown in Figure 18, the amount of DPIP transferred into AcLDL through the different DPIP microemulsions was higher than that through direct diffusion ( $27.70 \pm 1.99$  DPIP molecules /per AcLDL) and solubilization ( $66.97 \pm 1 4.81$  DPIP molecules /per AcLDL). Among the microemulsions studied, the seal oil microemulsion resulted in the highest amount of DPIP transferred into AcLDL ( $309.16 \pm 34.82$  vs  $151.31 \pm 28.54$  using triolein and  $203.19 \pm 64.51$  using squalene expressed as DPIP molecules/per AcLDL). The similar trend found in Figure 14 and Figure 18 suggests that the concentration of DPIP found in the microemulsion is the decisive factor for the transfer of the drug into AcLDL.

A possible explanation for these observations may lie in the differences in the physical behaviour of the different core lipids. Seal oil contains high levels of highly unsaturated triglycerides. These may allow for solvation of more hydrophobic DPIP than triolein and may also, because of increased fluidity, allow for more rapid transfer of DPIP to the lipoprotein particles.

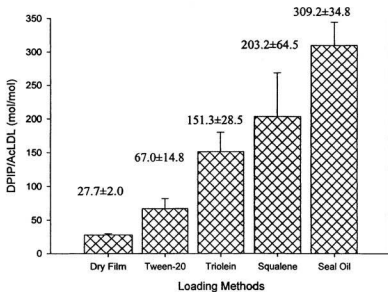


Figure 18. Comparison of the DPIP loading efficiency into AcLDL using different methods. Results are expressed as DPIP/AcLDL (mol/mol).

## **Conclusion**

To load DPIP into AcLDL, we prepared different DPIP microemulsions including the use of seal oil and squalene for the first time. We found that all DPIP microemulsions resulted in a higher DPIP incorporation into AcLDL than the two commonly used methods. More interestingly, DPIP microemulsion prepared using seal oil and squalene loaded more DPIP into AcLDL than that prepared using triolein, which is likely the result of the higher DPIP concentrations found in seal oil and squalene microemulsions. It is, therefore, suggested that seal oil and squalene may be used as substitutes for triolein in the manufacturing of microemulsions in pharmaceutical industry. Obviously significant studies, such as tests of safety and stability of these marine mammal oils, are required.

#### **Chapter 4. Incorporation of an <sup>125</sup>I-labeled hexa-iodinated diglyceride analog into low density lipoprotein and high specific uptake by cervical carcinoma cell lines<sup>\*\*\*</sup>**

##### **Introduction**

LDL is the predominant cholesterol transport vehicle in human blood. For each LDL particle, a hydrophilic shell surrounds approximately 1,500 molecules of cholesteryl esters in its lipophilic core. Tissue LDL uptake occurs through a pathway mediated by a specific cell surface LDL receptor. A protein unique to LDL particles, apo B-100, binds to this receptor, followed by cellular internalization and degradation of the particles. Cholesterol is then released for synthesizing and maintaining the various cell membranes (Brown and Goldstein, 1986). A number of tumor cell lines were found to have higher LDL receptor activity than normal cells (Ho et al., 1978; Gal et al., 1981; Vitols et al., 1985; Rudling et al., 1986; Rudling et al., 1990). Taking advantage of this preferential LDL accumulation, researchers have examined the utility of LDL as a vehicle for transporting cytotoxic drugs to tumor cells since 1981 (Gal et al., 1981; Iwanik et al., 1984; Masquelier et al., 1986; Lundbert, 1987; Vitols et al., 1990; Samadi-Baboli et al., 1990; Firestone, 1994). Although the usefulness of LDL as a carrier for antitumor agents has been extensively studied, little is known

---

<sup>\*\*\*</sup>Published in *Radiat. Res.*(see Xiao et al., 1999c)

regarding the accumulation of drug-LDL conjugates into tumors, and few animal or cancer patient studies were encouraging (De Smidt and van Berkel, 1990(a); Vitols et al., 1992; Ponty et al., 1993).

LDL has potential to also be an effective delivery vehicle of radiopharmaceuticals for tumor diagnosis and radiotherapy, because tumor cells have an elevated level of LDL receptors. This potential has generated some recent interest from researchers. There are two approaches to introduce radionuclides to LDL. One is to directly or indirectly link radionuclides, such as  $^{99m}\text{Tc}$ ,  $^{125}\text{I}$  or  $^{125}\text{I}$ -tyramine cellobiose, to apo B-100 of LDL (Ponty et al., 1993; Leppala et al., 1995; Pittman and Steinert, 1978). The other is to label LDL with a radionuclide through an LDL lipid-chelating agent (Jasanada et al., 1996; Urizzi et al., 1997). However, three major deficiencies of these approaches are that fixing radionuclides onto apo B-100 may impair its binding to the LDL receptor; few radioisotopes can be used to label LDL; and most LDL taken up by cells is degraded in the lysosomal compartment and metabolites are rapidly secreted from the cell. DPIP, a hexa-iodinated glyceride analog, was found to be resistant to lysosomal enzymes (Longino et al., 1983; Weichert et al., 1986; DeGalan et al., 1988) due to the presence of the ethyl group next to the ester bond. Therefore, in this study, we attempted to circumvent the deficiencies of labeling apo B-100 or LDL, by synthesizing DPIP, labeling it with  $^{125}\text{I}$ , and then incorporating it into LDL (forming  $^{125}\text{I}$ -DPIP-LDL conjugates) using a fusion technique. Three cervical cancer cell lines,

HeLa, SiHa, and C-33A, were used to evaluate the LDL receptor-mediated uptake of  $^{125}\text{I}$ -DPIP-LDL conjugates by cancer cells. The LDL receptor numbers and binding constants of SiHa and C-33A were also determined.

## **Materials and Methods**

### *Preparation of LDL, LPDS and AcLDL*

LDL and LPDS were isolated from human plasma (Canadian Red Cross, St. John's, Canada) by sequential density gradient ultracentrifugation, as previously described (Schumaker and Puppione, 1986), and stored at 4°C for up to two weeks. For the preparation of AcLDL, acetylation of LDL was performed, as described by Basu and coworkers (Basu et al., 1976). LDL, LPDS and AcLDL were dialyzed at 4°C for 16 hours in a buffer containing 0.3 mM EDTA, 150 mM NaCl and 50 mM Tris-HCl, at pH 7.4. For LDL receptor binding experiments, apo B-100 of LDL was labeled with  $^{125}\text{I}$  directly to its tyrosine residues by incubating LDL with Iodo-Beads (Pierce, Rockford, IL) in the presence of  $\text{Na}^{125}\text{I}$  at room temperature for 5 minutes.  $^{125}\text{I}$ -LDL was separated from free  $\text{Na}^{125}\text{I}$  by a Sephadex G-25 column.

### *Preparation of $^{125}\text{I}$ -DPIP-LDL*

DPIP was synthesized using previously reported methods (Longino et al., 1983) and labelled with  $^{125}\text{I}$  via an isotope exchange reaction with carrier free

aqueous Na<sup>125</sup>I (Mandel Scientific Company Ltd., Guelph, Canada) in pivalic acid (Aldrich Chemical Co., Burlington, Canada) (Weichert et al., 1986; DeGalan et al., 1988). The chemical and radiochemical purity of <sup>125</sup>I-DPIP thus obtained was determined by TLC and HPLC using a Beckman Gold system (Fullerton, CA) with a Phenomenex Bondclone10 C18 column (Torrance, CA).

To prepare <sup>125</sup>I-DPIP-LDL, <sup>125</sup>I-DPIP microemulsion was first prepared. 12 mg DPPC, 8 mg DPPE (Sigma Chemical Co., Burlington, Canada), 20 mg seal oil (Terra Nova Fishery, St. John's, Canada) and 10 mg <sup>125</sup>I-DPIP were dissolved in chloroform, dried under nitrogen flow, and suspended in 10 mL of saline. The suspension was sonicated for 2 hours at about -10°C under a nitrogen stream. The mixture was then centrifuged at 200,000g for 20 hours at 4°C. The floating microemulsion was collected.

<sup>125</sup>I-DPIP microemulsion was then incubated with LDL at 37°C for 24 hours at an <sup>125</sup>I-DPIP to LDL molar ratio of 1000:1. <sup>125</sup>I-DPIP-LDL was then purified by ultracentrifugation, as described previously (Schumaker and Puppione, 1986).

#### *Characterization of <sup>125</sup>I-DPIP-LDL*

The purity of <sup>125</sup>I-DPIP-LDL was analyzed by Sephadex G-25 chromatography in PBS. To assess and compare the integrity of apo B-100 in native LDL with that in LDL loaded with <sup>125</sup>I-DPIP, apo B-100 in both types of particles was analyzed by staining the bands obtained with SDS-PAGE. The effect of loading <sup>125</sup>I-DPIP on the

morphology of LDL particles was analyzed by EM, as described previously (Kader et al., 1998).

*Determination of receptor level, binding dissociation constant and cellular uptake of  $^{125}\text{I}$ -DPIP-LDL*

Exponentially growing HeLa, SiHa, and C-33A cells were maintained in Dulbecco's modified Eagle's medium containing 10% of fetal calf serum (FCS). The maximum LDL receptor number/cell ( $B_{\max}$ ) and binding dissociation equilibrium constant ( $K_d$ ) of LDL receptor were assayed, as described previously (Goldstein and Brown, 1974), with minor modification. To up-regulate the levels of LDL receptor,  $3 \times 10^5$  to  $10^6$  cells/well were plated into 8-well culture dishes and incubated in LPDS medium for 1 day for HeLa and C-33A or 2 days for SiHa. Then, cells were harvested at  $4^\circ\text{C}$  in various  $^{125}\text{I}$ -LDL concentrations in the absence or presence of 20-fold excess unlabeled LDL. After incubating HeLa and C-33A for 4 hours and SiHa for 8 hours, the cells were first washed thrice with 1 ml ice-cold 150 mM NaCl, 50mM Tris-HCl, pH 7.4, 2 mg/mL BSA and then thrice with 1 mL ice-cold PBS buffer. Cells were lysed in 1 ml of 0.1 M NaOH and the intracellular  $^{125}\text{I}$ -DPIP-LDL radioactivity was determined. Protein concentration assay was performed according to a method described by Bradford (Bradford, 1976). The  $B_{\max}$  and  $K_d$  for each cell line were determined using commercially obtained software (GraphPad Prism software<sup>®</sup> GraphPad Software Inc.). To determine whether LDL receptors mediated

the uptake, the same assays were used on cells grown for 4 hours at 37°C, as in the binding tests, in various concentrations of <sup>125</sup>I-DPIP-LDL, and in the absence or presence of 20-fold excess LDL specific competitor or AcLDL non-specific competitor.

## Results

DPIP was synthesized and labeled with <sup>125</sup>I. The maximum fraction of the input counts that bound to the cells was about 1/70 for C-33A cells, which have the highest level of LDL receptor expression. The labeling reaction was completed within 2 hours with little or no substrate decomposition. The radiochemical purity of <sup>125</sup>I-DPIP was found to be greater than 96%, based on the TLC and HPLC results (data not shown). <sup>125</sup>I-DPIP was then incorporated into LDL by our recently developed and highly efficient method using seal oil (Xiao et al., 1999b). Analyzed by column chromatography, the protein and radioactivity of the resultant product were found to overlap (Figure 19), suggesting that a stable <sup>125</sup>I-DPIP-LDL conjugate was formed. The loading efficiency for DPIP was found to be  $490 \pm 30$  molecules/LDL particle ( $n = 4$ ), which suggested that potentially as many as about 3,000 radiolabeled iodine atoms can be loaded into each LDL provided that the labeling efficiency is 100%. To characterize the integrity of apo B-100 and probably the whole LDL particle, <sup>125</sup>I-DPIP-LDL was compared with native LDL using SDS-PAGE. The only stained band

seen in both lanes was the apo B-100 band and neither had degradation products (data not shown).

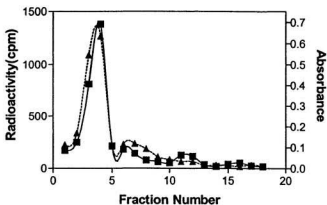


Figure 19. Confirmation of  $^{125}\text{I}$ -DPIP incorporation into LDL particles.  $^{125}\text{I}$ -DPIP-LDL conjugates were analyzed by gel filtration chromatography through Sephadex G-25 with PBS. Radioactivity (cpm, ■) and protein concentration, expressed in absorbance units, (▲) were analyzed, as described in the Materials and Methods

To evaluate *in vitro* receptor-mediated uptake of  $^{125}\text{I}$ -DPIP-LDL complex into cancer cells, we chose three cervical tumor cell lines, HeLa, SiHa, and C-33A. We first examined the maximum number of LDL receptors using  $^{125}\text{I}$ -LDL. The  $B_{\text{max}}$  was determined at  $4^{\circ}\text{C}$  to assay only binding and avoid the intracellular accumulation of  $^{125}\text{I}$ -LDL, recycling of LDL receptors or catabolism of  $^{125}\text{I}$ -LDL. Values were corrected for the non-specific binding of  $^{125}\text{I}$ -LDL to the cells when excess unlabeled LDL was added. HeLa cells were demonstrated to have a  $B_{\text{max}}$  value of  $38,300 \pm 9,800$  receptors/cell (Figure 20), similar to previous results (Lestavel-Delattre et al., 1992). The  $B_{\text{max}}$  values of SiHa and C-33A were found to be twice ( $B_{\text{max}} = 70,300 \pm 6,180$ ; Figure 21) and thrice ( $B_{\text{max}} = 120,000 \pm 22,800$ , Figure 22), respectively, as many as that of HeLa, indicating that these two cell lines are also good candidates for LDL-mediated cell-specific targeting of  $^{125}\text{I}$ -DPIP or other hydrophobic compounds using LDL (Table VII).

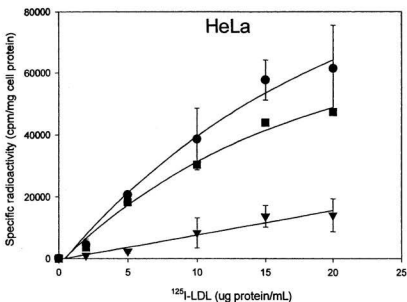


Figure 20. HeLa cell LDL receptor-mediated  $^{125}\text{I}$ -LDL binding. Binding assays of  $^{125}\text{I}$ -LDL to  $3 \times 10^5$  to  $10^6$  cells with incubation for 4 hours were at  $4^\circ\text{C}$  to avoid internalization or turnover. The total binding (cpm/mg protein cell extracts) was determined using no competitor (●), the nonspecific binding was determined using 20-fold excess unlabeled LDL (▼) and then the receptor-mediated binding was calculated by subtracting the nonspecific from total binding (■). Values are the mean  $\pm$  the standard error of the four independent experiments.

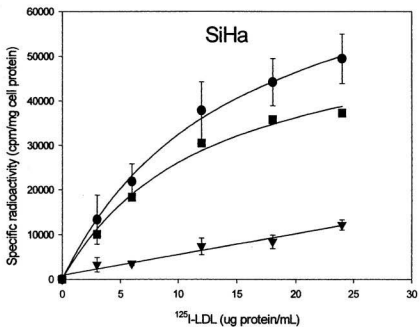


Figure 21. SiHa cell LDL receptor-mediated  $^{125}\text{I-LDL}$  binding. Conditions and labels were as for Figure 20.

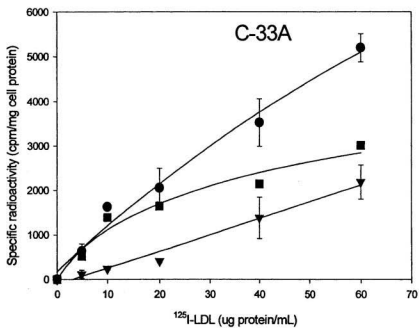


Figure 22. C-33A cell LDL receptor-mediated  $^{125}\text{I}$ -LDL binding. Conditions and labels were as for Figure 20.

Table VII. Maximum number of binding sites ( $B_{max}$ ) and equilibrium dissociation constant ( $K_d$ ) for LDL receptor-mediated binding of LDL to cervical cells

	HeLa	SiHa	C-33A
$B_{max}$	38,300 ± 9,900	70,300 ± 6,200	120,400 ± 21,800
$K_d$	34.0 ± 16.0	23.0 ± 4.4	49.9 ± 20.2

\*  $B_{max} \pm$  the standard deviation and  $K_d \pm$  the standard deviation were determined from the data of Figures 20-22.

To assess whether the uptake of  $^{125}\text{I}$ -DPIP-LDL was mediated by LDL receptors in HeLa, SiHa and C-33A cells, competition studies were conducted, as follows. Uptake of  $^{125}\text{I}$ -DPIP-LDL during incubation at  $37^\circ\text{C}$  with or without 20-fold excess native LDL was compared, and the nonspecific competition by LDL was assessed by the same experiment with or without AcLDL (Figure 23-25). Uptake of  $^{125}\text{I}$ -DPIP-LDL was significantly reduced by 20-fold excess native LDL for all three cell lines ( $p < 0.01$ ). We confirmed the previously reported findings (Goldstein et al., 1979) that  $^{125}\text{I}$ -DPIP-LDL uptake was specific for the LDL receptor pathway. We also found that  $^{125}\text{I}$ -DPIP-LDL uptake by HeLa, SiHa and C-33A cells was not competed ( $p > 0.05$ ) by AcLDL, which is not recognized by the LDL receptor.

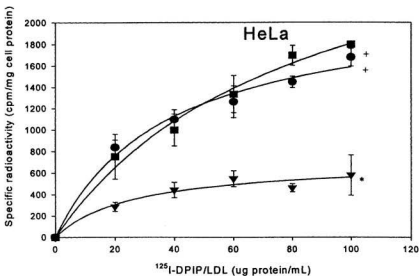


Figure 23. HeLa cell LDL receptor-mediated  $^{125}\text{I-DPIP-LDL}$  uptake. Cells were incubated at  $37^\circ\text{C}$  with  $^{125}\text{I-DPIP-LDL}$  complex with no competitor for the LDL receptor (●), 20-fold excess native LDL specific competitor (▼), or 20-fold excess AcLDL nonspecific competitor (■). Other conditions and labels were as for Figure 20. The p values were calculated from the results for all five concentrations in each curve using the matched pair test for each concentration. \*,  $p < 0.05$ ; +,  $p > 0.05$  for the difference between for each competition curve and the control curve. Other conditions and labels were as for Figure 20.

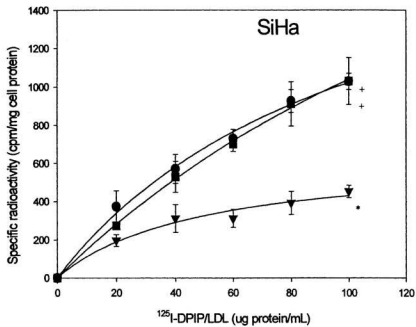


Figure 24. SiHa cell LDL receptor-mediated  $^{125}\text{I}$ -DPIP-LDL uptake. Conditions, labels and statistical analysis were as for Figure 23.

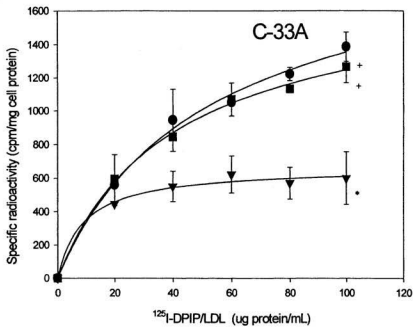


Figure 25. C-33A cell LDL receptor-mediated  $^{125}\text{I-DPIP-LDL}$  uptake. Conditions, labels and statistical analysis were as for Figure 23.

## Discussion

Imaging methods are important to clinicians in diagnosis of tumor or metastasis. Presently used tests have certain limitations and sometimes give false positive results. Although CT scanning and MRI have had wide application, many lesions cannot be further characterized with available imaging techniques. Also, these imaging tests often create new problems that require further investigation. Clearly, for common cancers, we require new screening tests that are specific but do not sacrifice sensitivity. Such imaging procedures should still provide diagnosis and follow-up of small lesions. Ideally, these new imaging methods would scan the whole body and be sensitive enough to detect lymph node and other metastases (Gucalp et al., 1997).

Several carrier systems, such as liposomes with or without antibodies, have been proposed for targeting radiopharmaceuticals to tumors for imaging or therapy (Carrasquillo, 1993). However, most carriers have problems. Carriers such as nanoparticles and liposomes fail to specifically target tumor cells (Lasic, 1996; Emmanuel et al., 1996). Shortcomings of immunocomplexes include their inability to target tumor cells *in vivo*, and the instability of surface antibodies or the antibody-containing conjugates (Mori and Huang, 1995). LDL is an endogenous lipid carrier that has also been proposed as a promising vehicle to carry drugs or diagnostic agents to cancer cells (Jasanada et al., 1996; Urizzi et al., 1997). The hydrophobic

core of LDL reportedly can hold many drug molecules (Vitols et al., 1990). In addition, most tumor cells divide rapidly and therefore have increased LDL receptor levels to supply cholesterol for their high level of membrane synthesis (De Smidt and van Berkel, 1990(b); Shaw et al., 1987; Filipowska et al., 1992). For example, cervical cancer cells take up 50-fold more LDL than normal gynecologic tissue (Gal et al., 1981a). During transport in the blood, lipids within LDL are also protected from enzymatic degradation, exchange with other lipoproteins, and dissociation from the complexes.

To develop radiopharmaceuticals for *in vivo* imaging, the high loading potential of LDL makes incorporating radioactive compounds into LDL an attractive alternative to labeling LDL directly. The major limitations of directly labeled LDL as a tumor imaging agent include inactivation of receptor-binding apo B-100 and low radioactive specific activity. In this study, radioiodinated DPIP was chosen for loading into LDL for the following reasons: 1) LDL native structure and function need to remain biochemically intact. Because DPIP is hydrophobic, it is likely to be stable in the lipophilic LDL core during transport in the blood. It should not disrupt the structure of the LDL particle and therefore binding of apo B-100 to the LDL receptor; 2) the ethyl group on the <sup>125</sup>I-DPIP side chain prevents cleavage of the ester bond by lysosomal enzymes. Consequently, the radioactive compound is also stable inside the cells (Longino et al., 1983). Further, our recent study of the biodistribution of an <sup>125</sup>I-labeled radiotracer, which has similar ester structure, in rabbits showed that it

remained intact (Xiao et al., 1999); 3) DPIP bears six iodine atoms on its aromatic rings for radiolabeling, which would result in high specific radioactivity; and 4) radioactive iodine isotopes meet the needs of most studies and clinical applications.  $^{131}\text{I}$  has been used most often for therapy or imaging (Carrasquillo, 1993).  $^{125}\text{I}$  or  $^{131}\text{I}$  can be used for experimental radiotherapy or radioimaging in small mammalian models, or experimental or applied therapy for humans. In addition,  $^{123}\text{I}$  can be used for imaging for humans.

One potential problem in using LDL as a carrier of drugs or diagnostic agents is the low incorporation efficiency of the drug molecules. In this study, we incorporated DPIP into LDL employing our recently developed novel method. We estimate that approximately 3,000 iodine atoms were incorporated into each LDL particle, which would provide sufficient radioactivity for most radioimaging applications, including the imaging of small primary tumors and metastases.

Cervical cancer is the second most common cancer of women in the world (Parkin et al., 1999). In this study, we chose three cervical tumor cell lines, HeLa, SiHa, and C-33A, to evaluate *in vitro* receptor-mediated uptake of  $^{125}\text{I}$ -DPIP-LDL complex. Cervical cancer cells have elevated LDL receptors that bind 15-fold to 30-fold more LDL than normal vital tissues, including the nonmalignant tissues most highly targeted by LDL, liver and adrenal gland (Gal et al., 1981b). HeLa is the cervical tumor cell line used most often for studies of anticancer drug-LDL complexes. HeLa cells were confirmed to have a high expression of LDL receptor, which was about 40,000 receptors per cell (Lestavel-Delattre et al., 1992; Figure 20,

Table VII). In this study, SiHa and C-33A were found to have higher LDL receptor expression than HeLa. The LDL receptor level was up-regulated by incubating cells in medium containing LPDS (Brown and Goldstein, 1976). We demonstrated that the uptake of  $^{125}\text{I}$ -DPIP-LDL was competed by native LDL, but not by AcLDL, suggesting that tumor cells took up  $^{125}\text{I}$ -DPIP-LDL through the LDL receptor pathway. Our results also suggested that LDL is a good vehicle to deliver  $^{125}\text{I}$ -DPIP to tumor cells and  $^{125}\text{I}$ -DPIP-LDL may be a promising tumor radioimaging agent. Our laboratory is further studying *in vivo* whole body imaging of tumor-bearing small animals using  $\gamma$ -scintigraphy.

## Chapter 5. Conclusion

LDL has been tested as a carrier for anti-cancer drug therapy for about twenty years. Although drug/LDL complexes have shown higher selectivity to tumor cells compared with the free drugs, their targeting effect is not high enough, in terms of the added toxicity to the anti-cancer drugs, to offset the cost of this delivery system. Because lowering the toxicity to normal cells, rather than increasing the toxicity to tumor cells, is the major concern of current cancer chemotherapy, drug-loaded LDL is thus not a feasible substitute for current formulations.

By contrast to cancer chemotherapy, since most radioimaging agents are non-toxic at their clinical dosage levels, incorporating appropriate radioimaging agents into LDL may take advantage of the selectivity of LDL to tumor cells without needing to consider the issue of toxicity to the normal tissues. This makes drug-loaded LDL a promising alternative to current tumor radioimaging drugs. In Chapter 4 of this thesis, we explored the potential of one drug/LDL complex as a promising cervical tumor imaging agent.

Radiolabeled LDL has been studied as an imaging agent for atherosclerosis for approximately the same length of time as LDL has been tested as an anti-cancer drug carrier. As indicated in Chapter 1, radioactivity on LDL will not stably locate at the lesion sites because apo B-100 protein, through which LDL binds cells, will be quickly degraded. Therefore, it is not readily to use LDL for detecting and monitoring plaques. In Chapter 2, which is the main part of this thesis, we combined the

achievements of the studies on using LDL as an anti-cancer drug carrier and using radiolabeled LDL as an imaging agent for atherosclerosis, and developed three imaging agents for atherosclerotic lesions by incorporating three non-hydrolyzable compounds into AcLDL. Our results demonstrated that radioimaging agent-loaded AcLDL has great potential for the purpose of atherosclerosis imaging. On the basis of the results in this thesis, further studies will be performed using other modified LDLs, such as OxLDL, methylated LDL, or glucosylated LDL, other radionuclides, such as  $^{99m}\text{Tc}$ ,  $^{123}\text{I}$ , or  $^{131}\text{I}$ , and other more potent compounds for both radioimaging and other imaging uses, including CT and MRI. We believe that clinical applications of our results will generate some positive outcomes.

## References

- Agatston A.S, Janowitz W.R, and Hildner F.J. Quantification of coronary artery calcium using ultrafast computed tomography. *J. Am. Coll. Cardiol.*; **15**: 827-832 (1990).
- Allison B.A., Crespo M.T., Jain A.K., Richter A.M., Hsiang Y.N. and Levy J.G. Delivery of benzoporphyrin derivative, a photosensitizer, into atherosclerotic plaque of Watanabe heritable hyperlipidemic rabbits and balloon-injured New Zealand rabbits. *Photochem. Photobiol.*; **65**(5): 877-883 (1997).
- Ambrose J.A. Angiographic correlations of advanced coronary lesions in acute coronary syndromes. In: Fuster V. ed. *Syndromes of atherosclerosis: correlations of clinical imaging and pathology*. Armonk, NY: Futura Publishing Company, Inc.: 105-122 (1996).
- Arnett E. N. , Isner M. , Redwood D. R. , Kent K. M. , Daker W. P. , Ackerstien H. and Roberts W. C. . Coronary artery narrowing in coronary heart disease: Comparison of cineangiographic and necropsy findings. *Ann. Int. Med.* **91**: 350-356 (1979).
- Atsma D. E. , Feitsma R. I. , Camps J. , van 't Hooft F. M. , van der Wall E. E., Nieuwenhuizen W. and Pauwels E. K. J. . Potential of <sup>99m</sup>Tc-LDLs labeled by two different methods for scintigraphic detection of experimental atherosclerosis in rabbits. *Arterioscler. Thromb.* **13**: 78-83 (1993).
- Basu S. K., Goldstein J. L. , Anderson R. G. W. , Brown, M. S. Degradation of

- cationized low density lipoprotein and regulation of cholesterol metabolism in homozygous familial hypercholesterolemic fibroblasts. *Proc. Natl. Acad. Sci. USA* **73**; 3178-3182 (1976).
- Bonaa K. H. , Bjerve K. S., Straume B., Gram T. T. and Thelle D.. Effect of Eicosapentaenoic and docosahexaenoic acids on blood pressure in hypertension. A population-based intervention trial from the Tromso study. *N. Eng. J. Med.* **322**: 795-801 (1990).
- Bradford M. M. A rapid and sensitive method for the quantitation of microgram quantities of protein utilizing the principle of protein dye binding. *Anal. Biochem.* **72**: 248 (1976).
- Brown M. S. and Goldstein J. L. Receptor-mediated control of cholesterol metabolism. *Science* **191**: 150-154 (1976).
- Brown M. S. and Goldstein J. L. . Lipoprotein metabolism in the macrophage: implications for cholesterol deposition in atherosclerosis. *Annu. Rev. Biochem.* **52**: 223-261 (1983).
- Brown M. S. and Goldstein J. L. , A receptor-mediated pathway for cholesterol homeostasis. *Science* **232**: 34-47 (1986).
- Buja L. M. , Kita T. , Goldstein J. L. , Watanabe Y. and Brown M. S. . Cellular pathology of progressive atherosclerosis in the WHHL rabbit. An animal model of familial hypercholesterolemia. *Arteriosclerosis* **3**: 87-101 (1983)
- Cardin A. D. , Price C. A. , Hirose N. , Krivanek M. A., Blankenship D. T. , Chao J. and Mao S. J. T.. Structural organization of apolipoprotein B-100 of human

- plasma low density lipoproteins. Comparison to B-48 of chylomicrons and very low density lipoproteins. *J. Biol. Chem.* **261**: 16,744-16,748 (1986).
- Carrasquillo, J. Imaging and dosimetry determinations using radiolabeled antibodies. *Cancer Treat. Res.* **68**: 65-97 (1993).
- Carrio I. Pieri P. and Prat L. In-111 chimeric negative-charged Z2D3 PL-F(ab')<sub>2</sub> in the detection of atherosclerotic plaques [Abstract]. *J. Nucl. Med.* **36**: 133P (1995).
- Chang M.Y., Lees A.M, and Lees R.S. Time course of 125I-labeled LDL accumulation in the healing, balloon-deendothelialized rabbit aorta. *Arteriosclero Thromb*; **12**: 1088-1098 (1992).
- Chang M.Y., Lees A.M., and Lees R.S. Low density lipoprotein modification and arterial wall accumulation in a rabbit model of atherosclerosis. *Biochemistry*; **32**: 8518-8524 (1993).
- Christensen M. S., Hoy C. E., Redgrave T. G. Lymphatic absorption of n-3 polyunsaturated fatty acids from marine oils with different intramolecular fatty acid distributions. *Biochim. Biophys. Acta* **1215**: 198-204 (1994).
- Christensen M. S. and Hoy C. E. . Effects of dietary triacylglycerol structure on triacylglycerols of resultant chylomicrons from fish oil- and seal oil-fed rats. *Lipids* **31**: 341-344 (1996).
- De Smidt P.C., and van Berkel T. J. C., Prolonged serum half-life of antineoplastic drugs by incorporation into the low density lipoprotein. *Cancer Res.* **50**; 7476-7482 (1990a).

- De Smidt P. C. and van Berkel T. J. C. LDL-mediated drug targeting. *Crit. Rev. Ther. Drug Carriers Syst.* **7**: 99-119 (1990b).
- DeForge LE, Schwendner SW, DeGalan MR, McConnell DS and Counsell RE. Noninvasive assessment of lipid disposition in treated and untreated atherosclerotic rabbits. *Pharmaceut. Res.* **6**: 1011-1015 (1989).
- DeForge L., DeGalan M. R., Ruyan M. K., Newton R. S., and Counsell R. E. Comparison of methods for incorporating a radioiodinated residualizing cholesteryl ester analog into low density lipoprotein. *Nucl. Med. Biol.* **19**: 775-782 (1992).
- DeGalan M.R., Schwendner S.W., Weichert J.P. and Counsell R.E. Radioiodinated cholesteryl iopanoate as a potential probe for the *in vivo* visualization of atherosclerotic lesions in animals. *Pharmaceut. Res.*; **3**: 52-55 (1986).
- DeGalan M. R. , Schwendner S. W., Skinner R. W. S. , Longino M. A., Gross M. and Counsell R. E. . Iodine-125 cholesteryl iopanoate for measuring extent of atherosclerosis in rabbits. *J. Nucl. Med.* **29**: 503-508 (1988).
- Den Heijer P, Foley D.P., and Hillege H.L. The "Erminonville" classification of observations at coronary angiography: evaluation of intra- and inter-observer agreement. *Eur. Heart J.*; **15**: 815-822 (1994).
- Dinkelborg L.M., Hilger C.S., and Semmier W. Endothelin derivatives for imaging of atherosclerosis. *J. Nucl. Med.* **36**: 102P (1995).
- Dinsmore R.E., and Rivitz S.M.. Imaging techniques in carotid and peripheral vascular disease. In: Fuster V. ed. *Syndroms of atherosclerosis: correlation*

- of clinical imaging and pathology*. Armonk, NY: Futura Publishing Company, Inc. 277-289 (1996).
- Doyle M. and Pohost G. Magnetic resonance coronary artery imaging. In: Fuster V. ed. *Syndromes of atherosclerosis: correlations of clinical imaging and pathology*. Armonk, Ny: Futura Publishing Company, Inc. 313-332 (1996).
- Eliasziw M, Rankin M.B, and Fox A.J. Accuracy and prognostic consequences of ultrasonography in identifying severe carotid stenosis. *Stroke*; 26: 1747-1752 (1995).
- Emmanuel N. , Kedar E. , Bolotin E. M. , Smorodinsky N. I., Berenholz, Y. Targeted delivery of doxorubicin via sterically stabilized immunoliposomes: pharmacokinetics and biodistribution in tumor bearing mice. *Pharm. Res.* 13, 861-868 (1996).
- Falk E., Shah, P.K., and Fuster V. Coronary plaque disruption. *Circulation*; 92: 657-671 (1995).
- Falk E, and Fernandez-Ortiz A. Role of thrombosis in atherosclerosis and its complications. *Am. J. Cardiol.* ; 75: 5B-11B (1995).
- Filipowska D., Filipowski T. , Morelowska B., Kazanowska W., Laudanski T., Lapinjoki S., Akertland M., and Breeze, A. Treatment of cancer patients with a low density lipoprotein delivery vehicle containing a cytotoxic drug. *Cancer Chemother. Pharmacol.* 29: 396-400 (1992).
- Firestone R.A. Low-density lipoprotein as a vehicle for targeting antitumor compounds to cancer cells. *Bioconjugate Chem.* 5: 105-113 (1994).

- Fischman A.J, Rubin R.H, and Khaw B.A. Radionuclide imaging of experimental atherosclerosis with nonspecific polyclonal immunoglobulin G. *J. Nucl. Med.*; **30**: 1095-1100 (1989).
- Fox P. L. and DiCorleto P. E.. Fish oils inhibit endothelial cell production of platelet-derived growth factor-like proteins. *Science* **241**: 453-466 (1988).
- Gal D., Ottashi M., MacDonald P. C., Buschbaum H. J. , and Simpson E. R. , Low density lipoprotein as a potential vehicle for chemotherapeutic agents and radionucleotides in the management of gynecologic neoplasms. *Amer. J. Obstet. Gynecol.* **139**: 877-885 (1981a).
- Gal D., MacDonald P. S., Porter J. C., Smith J. W., and Simpson E. R. Effect of cell density and confluency on cholesterol metabolism in cancer cells in monolayer culture. *Cancer Res.*, **41**: 473-477 (1981b).
- Galis Z.S, Galina Sukhova G.K, and Kranzhofer R. Macrophage foam cells from experimental atheroma constitutively produce matrix-degrading proteinases. *Proc. Natl. Acad. Sci. USA*; **92**: 402-406 (1995).
- Gerrity R. G. . The role of the monocyte in atherogenesis. I. Transition of blood-borne monocytes into foam cells in fatty lesions. *Am. J. Pathol.* **103**: 181-190 (1981).
- Ginsberg H.N., goldsmith S.J. and Vallabhajosula S. Non-invasive imaging of <sup>99m</sup>technetium-labeled low density lipoprotein uptake by tendon xanthomas in hypercholesterolemic subjects. *Arteriosclerosis*; **10**: 256-262 (1990).
- Goldstein J. L., and Brown M. S. Binding and degradation of low density

- lipoproteins to cultured human fibroblasts. *J. Biol. Chem.* **249**: 5153-5162 (1974).
- Goldstein J. L., Ho Y. K., Basu S. K. and Brown M. S. Binding site on macrophages that mediates uptake and degradation of acetylated low density lipoprotein, producing massive cholesterol deposition. *Proc. Natl. Acad. Sci. USA.* **76**: 333-337 (1979).
- Grist T. and Turski P.A. Nuclear magnetic resonance imaging as applied to carotid and peripheral atherosclerotic vascular disease. In: Fuster V. ed. *Syndromes of atherosclerosis: correlations of clinical imaging and pathology.* Armonk, NY: Futura Publishing Company, Inc.; 333-362 (1996).
- Gucalp R., Dutcher J. P., and Wiernik, P. H. Overview by an oncologist: what are the imaging needs of the oncologist and oncological surgeon? *Semin. Nucl. Med.* **27**: 3-9 (1997).
- Hardoff R, Braegelmann F. and Zanzanico P. External imaging of atherosclerosis in rabbits using an <sup>123</sup>I-labeled synthetic peptide fragment. *J. Clin. Pharmacol.* **33**: 1039-1047 (1993).
- Harris W. S., Zucker M. L. and Dujovne C. A. Omega-3 fatty acids in hypertriglyceridemic patients: triglycerides vs. methyl esters. *Am. J. Clin. Nutr.* **48**: 992-997 (1988).
- Ho Y. K., Smith G. S., Brown M. S., and Goldstein J. L. Low density lipoprotein (LDL) receptor activity in human myelogenous leukemia cells. *Blood* **52**: 1099-1104 (1978).

- Iwanik M. , Shaw K.V., Ledwith B. , Yanovich S. , and Shaw J. M. Preparation and interaction of a low density lipoprotein: daunomycin complex with P388 leukemic cells. *Cancer Res.*, **44**: 1206-1215 (1984).
- Janowitz W.R, Agaiston A.S, Kaplan G, and Viamonte M Jr. Differences in prevalence and extent of coronary calcium detected by ultrafast computed tomography in asymptomatic men and women. *Am J. Cardiol.*; **72**: 247-254 (1993).
- Jasanada F. , Urizzi P., Souchard J. P., Le Gaillard F., Favre G. , and Nepveu F. Indium-111 labeling of low density lipoproteins with the DTPA-bis (stearylamine): evaluation as a potential radiopharmaceutical for tumor localization. *Bioconjug. Chem.* **7**: 72-81 (1996).
- Kaartnen M. Penttila A., and Kovanen PT. Accumulation of activated mast cells in the shoulder region of human coronary atheroma, the predilection site of atheromatous rupture. *Circulation* **90**: 1669-1678 (1994).
- Kader A., Davis P. J., Kara M., Liu H. Drug targeting using low density lipoprotein (LDL): physicochemical factors affecting drug loading into LDL particles. *J. Controlled Release* **55**: 231-243 (1998)
- Kenji I., Toru K., Noriaki K., Yutaka N. and Chuichi K. Uptake of acetylated LDL by peritoneal macrophages obtained from normal and Watanabe heritable hyperlipidemic rabbits, an animal model for familial hypercholesterolemia. *Biochim. Biophys. Acta.* **962**: 387-389 (1988).
- Kessel D. and Sykes F. Porphyrin accumulation by atheromatous plaque of the

- aorta. *Photochem. Photobiol.* **40**: 59-62 (1984).
- Kohler T.R. Imaging of carotid artery lesions: a surgeon's view. In: Fuster V. ed. *Syndromes of atherosclerosis: correlations of clinical imaging and pathology.* Armonk, NY: Futura Publishing Company, Inc.: 205-223 (1996).
- Kritz H., Underwood S.R. and Sinzinger H. Imaging of atherosclerosis (part II). *Wien Klin Wochenschr* **108**: 87-97 (1996).
- Kubota R. Kubota K, and Yamada S. Microautoradiographic study for the differentiation of intratumoral macrophages, granulation tissues and cancer cells by the dynamics of fluorine-18-fluorodeoxyglucose uptake. *J. Nucl. Med.*; **35**: 104-112 (1994).
- Lasic D. D. Doxorubicin in sterically stabilized liposomes. *Nature* **380**: 561-562 (1996).
- Lees A. M. , Lees R. S., Schoen F. J., Issacsohn J. L., Fischman A. J., McKusick K. A. and Strauss H. W. Imaging human atherosclerosis with <sup>99m</sup>Tc-labeled low density lipoprotein. *Atherosclerosis* **8**: 461-470 (1988).
- Lees R.S., and Lees A.M. Radiopharmaceutical imaging of atherosclerosis. In: Fuster V. ed. *Syndromes of atherosclerosis: correlations of clinical imaging and pathology.* Armonk, Ny: Futura Publishing Company, Inc.:385-401 (1996).
- Lees A.M., Lees R.S., and Schoen F.J. Imaging human atherosclerosis with <sup>99m</sup>Tc-labeled low density lipoprotein. *Atherosclerosis* **8**: 461-468 (1988).
- Lees R.S, Lees A.M, and Strauss H.W. External imaging of human atherosclerosis.

- J. Nucl. Med.* **24**: 154-156 (1983).
- Lees R. S. , Garabedian H. D., Lees A. M., Schumacher D. J., Miller A., Isaacsohn J. L., Derksen A. and Strauss H. W. Technetium-99m low density lipoprotein: Preparation and biodistribution. *J. Nucl. Med.* **26**: 1056-1062 (1985).
- Leppala L., Kallio M., Nikula T., Nikkinen P., Liewendahl K., Jaaskelainen J., Savolainen S., Gylling H., Hiltunen J., Callaway J., Kahl S., and Farkkila M. Accumulation of <sup>99m</sup>Tc-low-density lipoprotein in human malignant glioma. *Br. J. Cancer*, **71**: 383-387 (1995).
- Lestavel-Delattre S., Martin-Nizard F., Clavey V., Testard P., Favre G., Doualin G., Houssaini H. S., Bard J., Duriez P., Delbart C., Soula G., Lesieur D., Lesieur I., Cazin J., Cazin M., and Fruchart, J. Low-density lipoprotein for delivery of an acrylophenone antineoplastic molecule into malignant cells. *Cancer Res.* **52**: 3629-3635 (1992).
- Liu F. and Liu D. Long-circulating emulsions (oil-in-water) as carriers for lipophilic drugs. *Pharm. Res.* **12**: 1060-1064 (1995).
- Longino M. A., Weichert J. P., Schwendner S. W., Szabo S. M., Counsell R. E. and Glazer G. M. Biodistribution of a new lipid-soluble CT contrast agent. Evaluation of cholesteryl iopanoate in the rabbit. *Invest. Radiol.* **18**: 275-278 (1983).
- Luliano L., Signore A. and Vallabhajosula S. Preparation and biodistribution of <sup>99m</sup>technetium-labeled oxidized LDL in man. *Atherosclerosis*; **126**:131-141

(1996).

- Lundberg B. Preparation of drug-low density lipoprotein complexes for delivery of antitumoral drugs via the low density lipoprotein pathway. *Cancer Res.* **47**: 4105-4108 (1987).
- Masquelier M., Vitols S., and Peterson C. O. Low density lipoprotein as a carrier of antitumoral drugs: *in vivo* fate of drug-human low-density lipoprotein complexes in mice. *Cancer Res.* **46**: 3842-3847 (1986).
- Maximilian L.B, and Willerson J.T. Role of inflammation in coronary plaque disruption. *Circulation*; **89**: 503-505 (1994).
- Moreno P.R, Falk E, and Palacios I.F. Macrophage infiltration in acute coronary syndromes. *Implications Plaque Rupture Circ.* **90**: 775-778 (1994).
- Mori A. and Huang L. Targeted Immunoliposomes: potential role in the delivery of cytotoxic drugs. *Clin. Immunother.* **3**: 227-240 (1995).
- Narula J. Petrov A. and Bianchi C. Noninvasive localization of experimental atherosclerotic lesions with mouse/human atheroma imaging with conventional and negative charge-modified antibody fragments. *Circulation* **92**: 474-484 (1995).
- Narula J., Petrov A., Pak K.Y., Ditlow C., Chen F. and Khaw B. A. Noninvasive detection of atherosclerotic lesions by <sup>99m</sup>Tc-based immunoscintigraphic targeting of proliferating smooth muscle cells. *Chest* **111**: 1684-1690 (1997).
- Nicolas J. M., Leclef B. , Jardez H., Keyeux A., Melin J A. and Trouet A. Imaging atherosclerotic lesions with <sup>111</sup>In-labeled low density lipoprotein. (abstract)

Vienna. *Proceedings of the International Atherosclerosis Congress*. p A219 (1989).

Nissen S.E., Tuzcu E.M., and DeFranco A.C. Detection and quantification of atherosclerosis: the emerging role of intravascular ultrasound. In: Fuster V. ed. *Syndromes of atherosclerosis: correlations of clinical imaging and pathology*. Armonk, NY: Futura Publishing Company, Inc.: 291-312 (1996).

Osterud B., Elvevoll E., Barstad H., Brox J., Halvorsen H., Lia K., Olsen J. O., Olsen R. L., Sissener C. and Rekdal O. Effect of marine oils supplementation on coagulation and cellular activation in whole blood. *Lipids* **30**: 1111-1118 (1995).

Parkin D. M., Pisani P., Ferlay J. Estimates of the worldwide incidence of 25 major cancers in 1990. *Int. J. Cancer*. **80**: 827-841 (1999).

Phelps M.E., Hoffman E.J., and Selin C. Investigation of <sup>18</sup>F-2-deoxyglucose for the measurement of myocardial glucose metabolism. *J. Nucl. Med.* **19**: 1311-1319 (1978).

Pirch C., and Sinzinger H. Evidence for lipid regression in humans in vivo performed by <sup>123</sup>I-low density lipoprotein scintiscanning. *Ann NY Acad Sci*; **748**: 613-621 (1995).

Pittman R. C., and Steinberg D. A new approach for assessing cumulative lysosomal degradation of proteins and other macromolecules. *Biochem. Biophys. Res. Commun.* **81**: 1254-1259 (1978)

Ponty E., Favre G., Benaniba R., Boneu A., Lucot H., Carton M., and Soula, G.

- Biodistribution study of  $^{99m}\text{Tc}$ -labeled LDL in B16-melanoma-bearing mice: Visualization of a preferential uptake by the tumor. *Int. J. Cancer* **54**: 411-417 (1993).
- Prat L. Torres G. and Carrio I. Polyclonal  $^{111}\text{In}$ -IgG,  $^{125}\text{I}$ -LDL and  $^{125}\text{I}$ -endothelin-1 accumulation in experimental arterial wall injury. *Eur. J. Nucl. Med.* **20**: 1141-1145 (1993).
- Redgrave, T.G. and Maranhao, R.C. Metabolism of protein-free lipid emulsion models of chylomicrons in rats. *Biochim. Biophys. Acta* **835**: 104-112 (1985).
- Roberts A. B., Lees A. M., Lees R. S., Strauss H. W., Fallon J. T., Taveras J. and Kapiwoda S. Selective accumulation of low density lipoproteins in damaged arterial wall. *J. Lipid Res.* **24**: 1160-1167 (1983).
- Roelandt J.R.T.C., Di Mario C., and Pandian N.G. Three-dimensional reconstruction of intracoronary ultrasound images: rationale, approaches, problems and directions. *Circulation* **90**:1044-1055 (1994).
- Rosen J. M., Butler S. P., Meinken G. E., Wang T. S. T., Ramakrishan R., Srivastava S. C., Alderson P. O. and Ginsberg H. N. Indium-111 labeled LDL: A potential agent for imaging atherosclerotic disease and lipoprotein distribution. *J. Nucl. Med.* **31**: 343-350 (1990).
- Ross, R. The pathogenesis of atherosclerosis: a perspective for the 1990s. *Nature*; **362**: 801-809 (1993).
- Rudling M. J., Stihle L., Peterson C. O., and Skoog L., Content of low density lipoprotein receptors in breast cancer tissue related to survival of patients.

- Brit. Med. J.* **292**: 580-582 (1986).
- Rudling M. J., Angelin B. C., Peterson O., and Collins V. P. Low density lipoprotein receptor activity in human intracranial tumors and its relation to the cholesterol requirement. *Cancer Res.* **50**: 483-487 (1990).
- Samadi-Baboli M., Favre G., Bernadou J., Berg D., and Soula G. Comparative study of the incorporation of ellipticine-esters into low density lipoprotein (LDL) and selective cell uptake of drug-LDL complex via the LDL receptor pathway *in vitro*. *Biochem. Pharmacol.* **2**: 203-212 (1990).
- Samadi-Baboli M., Favre G., Canal P. and Soula G. Low density lipoprotein for cytotoxic drug targeting: improved activity of elliptinium derivative against B16 melanoma in mice. *Br. J. Cancer* **68**: 319-326 (1993).
- Schumaker V. N. and Puppione D. L. Sequential flotation ultracentrifugation. *Methods in Enzymology* **128**: 155-171 (1986).
- Schwartz C. J., Valente A. J., Sprague E. A., Kelley J. L., and Nerem R. M. The pathogenesis of atherosclerosis, an overview. *Clin. Cardiol.* **14**: I-1 - I-16 (1991).
- SeEVERS R. H., Groziak M. P., Weichert J. P., Schwendner S. W., Szabo S. M., Longino M. A. and Counsell R. E. Potential tumor- or organ-imaging agents. 23 Sterol esters of iopanoic acid. *J. Med. Chem.* **25**: 1500-1503 (1982).
- Shaw J. M., Shaw K.V., Yanovich S., Iwanik M. , Futch, W. S. A. Rosowsky, and L. B. Schook, Delivery of lipophilic drugs using lipoproteins. *Ann. N. Y. Acad. Sci.* **507**: 252-271 (1987).

- Shih I-L., Lees R.S., Chang M.Y., and Lees A.M. Focal accumulation of an apolipoprotein B-based synthetic oligopeptide in the healing rabbit arterial wall. *Proc Natl Acad Sci USA* **87**: 1436-1440 (1990).
- Simopoulos A. P. Omega-3 fatty acids in health and disease and in growth and development. *Am. J. Clin. Nutr.* **54**: 438-463 (1991).
- Sinzinger H., Bergmann H., Kaliman J., and Angelberger P.. Imaging of human atherosclerotic lesions using  $^{123}\text{I}$ -low density lipoprotein. *Eur. J. Nucl. Med.* **12**: 291-292 (1986).
- Sinzinger H. and Angelberger P. Imaging and kinetic studies with radiolabeled autologous low-density-lipoproteins (LDL) in human atherosclerosis. *Nucl. Med. Comm.* **9**: 859-866 (1988).
- Sinzinger H. and Virgolini I. Nuclear medicine and atherosclerosis. *Eur. J. Nucl. Med.*; **17**: 160-178 (1990).
- Sinzinger H., Rodrigues M. and Kritz H. Radioisotopic imaging of atheroma. In: Fuster V. ed. *Syndromes of atherosclerosis: correlations of clinical imaging and pathology*. Armonk, Ny: Futura Publishing Company, Inc. 369-383 (1996).
- Skinner M.P., Yuan C. and Mitsumori L. Serial MRI of experimental atherosclerosis detects lesion fine structure, progression and complications *in vivo*. *Nat. Med.* **1**: 69-73 (1995).
- Spokojny, A.M., Serur J.R., Skillman J. and Spears J.R. Uptake of hematoporphyrin derivative by atheromatous plaques: studies *in vitro* and in rabbits *in vivo*. *J.*

- Am. Coll. Cardiol.*; **8**: 1387-1392 (1986).
- Sqalli-Houssaini H., Pierlot C., Kusnierz J-P., Parmentier B., Martin-Nizard F., Lestavel-Delattre S., Tartar A., Fruchart J-C., Sergheraert C. and Duriez P. Preparation of anti-HIV-low-density lipoprotein complexes for delivery of anti-HIV drugs via the low-density lipoprotein pathways. *Biotechnol. Ther.* **5**: 69-85 (1994).
- Stary H.C, Chandler A.B., and Glagov S. A definition of initial, fatty streak, and intermediate lesions of atherosclerosis. A report from the committee on vascular lesions of the Council on Arteriosclerosis, American Heart Association. *Arterioscler Thromb*; **14**: 840-856 (1994).
- Stary H.C., Chandler A.B., and Dinsmore R.E. A definition of advanced types of atherosclerotic lesions and a histological classification atherosclerosis. A report from the committee on vascular lesions of the Council on Arteriosclerosis, American Heart Association. *Arterioscler Thromb*; **15**:1512-1531 (1995).
- Strauss W.H. Imaging atherosclerosis: a worthy challenge. *J. Nucl. Cardiol.* **3**: 278-280 (1996).
- Strauss L.G. and Conti P.S. The applications of PET in clinical oncology. *J. Nucl. Med.* **32**: 623-648 (1991).
- Uchida Y., Nakamura F., and Tomaru T. Prediction of acute coronary syndromes by percutaneous coronary angiography in patients with stable angina. *Am. Heart J.* **130**: 195-203 (1995).

- Urizzi P., Souchard J. P., Palevody C., Ratovo G., Hollande E., and Nepveu F. Internalization of indium-labeled LDL through a lipid chelating anchor in human pancreatic-cancer cells as a potential radiopharmaceutical for tumor localization. *Int. J. Cancer*, **70**: 315-322 (1997).
- Vallabhajosula J., Machac K. and Knesaurek J. Imaging atherosclerotic macrophage density by positron emission tomography using F-18-fluorodeoxyglucose (FDG) *J. Nucl. Med.* **37**: 38p (1996).
- Vallabhajosula S. and Goldsmith S.J. <sup>99m</sup>Tc-low density lipoprotein: intracellularly trapped radiotracer for non-invasive imaging of LDL metabolism *in vivo*. *Semin Nucl. Med.* **20**: 68-79 (1990).
- Vallabhajosula S., Paidi M. and Badimon J.J. Radiotracers for low density lipoprotein biodistribution studies *in vivo*: technetium-99m low density lipoprotein versus radioiodinated low density lipoprotein preparations. *J. Nucl. Med.* **29**: 1237-1245 (1988).
- Vallabhajosula S., Ali K.S.M. and Goldsmith S.J. Evaluation of Tc-99m-labeled peptides for imaging atherosclerotic lesions *in vivo*. *J. Nucl. Med.* **34**: 66P (1993)
- Virgolini I., Rauscha F. and Lupattelli G. Autologous low-density lipoprotein labeling allows characterization of human atherosclerotic lesions *in vivo* as to presence of foam cells and endothelial coverage. *Eur J. Nucl. Med.* **18**: 948-951 (1991).
- Vitols S., Gahrton G., Bjorkholm M., and Peterson C. O. Hypocholesterolemia in

malignancy due to elevated LDL receptor activity in tumor cells: evidence from studies in leukemic patients. *Lancet* II: 1150-1154 (1985).

Vitols S., Soderberg-Reid K., Masquelier M., Sjostrom B., and Peterson C. O. Low density lipoprotein for delivery of a water insoluble alkylating agent to malignant cells. *In vitro* and *in vivo* studies of drug-lipoprotein complex. *Brit. J. Cancer* 62: 724-729 (1990).

Vitols S., Peterson C., Larsson O., Holm P., and Aberg B. Elevated uptake of low density lipoproteins by human lung cancer tissue *in vivo*. *Cancer Res.* 52: 6244-6247 (1992).

Vlodaver Z., Frech R., Van Tassel R. A., and Edwards J. E. Correlation of the antmortem coronary arteriogram and the postmortem specimen. *Circulation* 47: 162-169 (1973).

Von Birgelen C., Slager C.J., and Mario C.D. Intra-coronary ultrasound: a new maximum confidence approach for the quantitative assessment of progression-regression of atherosclerosis? *Atherosclerosis* 118:S103-S113 (1995).

Weichert J. P., Groziak M. P., Longino M. A., Schwendner S. W, and Counsell R. E. Potential tumor or organ-imaging agents. 27. Polyiodinated 1,3-disubstituted and 1,2,3-trisubstituted triacylglycerols. *J. Med. Chem.* 29: 2457-2465 (1986).

Weichert J. P., Longino M. A., Bakan D. A., Spigarelli M. G., Chou T-S., Schwendner S. W. and Counsell R. E. Polyiodinated triglyceride analogs as

- potential computed tomography imaging agents for the liver. *J. Med. Chem.* **38**: 636-646 (1995).
- Wexler L., Brundage B., and Crouse J. Coronary artery calcification: pathophysiology, epidemiology, imaging methods and clinical implications. *Circulation* **94**: 1175-1192 (1996).
- Xiao W., Wang L., Scott T.M., Counsell R.E. and Liu H. Radiolabeled cholesteryl iopanoate/acetylated low density lipoprotein as a potential probe for visualization of early atherosclerotic lesions in rabbits. *Pharmaceut. Res.* **16**: 420-426, (1999a).
- Xiao W., Wang L., Davis P.J. and Liu H. Seal oil markedly enhances the transfer of a hydrophobic radiopharmaceutical into acetylated low density lipoprotein. *Lipids.* **34**(5): 503-509, (1999b).
- Xiao W., Wang L., Ryan J.M., Pater A. and Liu H. Incorporation of an <sup>125</sup>I-labeled hexa-iodinated diglyceride analog into low density lipoprotein and high specific uptake by cervical carcinoma cell lines. *Radiat. Res.* **152** (3): 250-256, (1999c).
- Yancey P.G. and Jerome W.G. Lysosomal sequestration of free and esterified cholesterol from oxidized low density lipoprotein in macrophages of different species. *J. of Lipid Res.* **39**: 1349-1361 (1998).
- Yla-Hertuala S., Rosenfeld M. E., Parthasarathy S., Sigal E., Sarkioja T., Witztum J. L., and Steinberg D. Gene expression in macrophage-rich human atherosclerotic lesions. 15-lipoxygenase and acetyl low density lipoprotein

receptor messenger RNA colocalize with oxidation specific lipid-protein adducts. *J. Clin. Invest.* **87**: 1146-1152 (1991).

